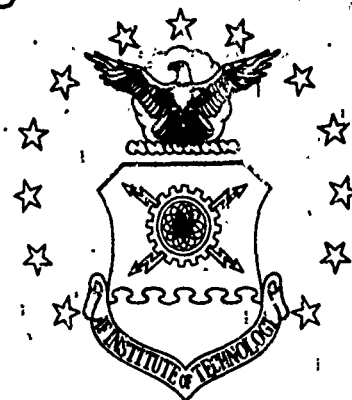
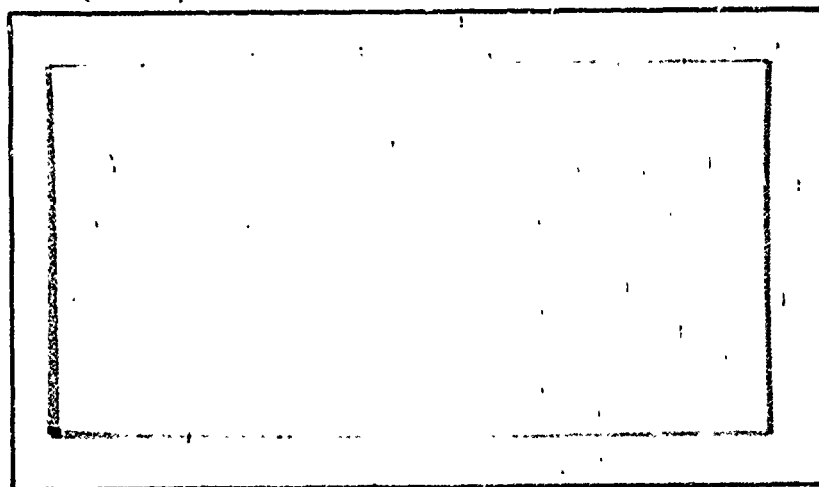


AD 744816

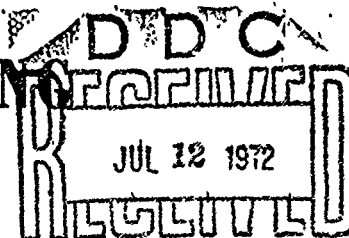
AIR FORCE INSTITUTE OF TECHNOLOGY



AIR UNIVERSITY
UNITED STATES AIR FORCE



SCHOOL OF ENGINEERING



WRIGHT-PATTERSON AIR FORCE BASE, OHIO

Reproduced by
NATIONAL TECHNICAL
INFORMATION SERVICE
U S Department of Commerce
Springfield VA 22151

10

DOCUMENT CONTROL DATA - R & D

(Security classification of title, body of abstract and indexing annotation must be entered when the overall report is classified)

ORIGINATING ACTIVITY (Corporate author)

AFIT-EN

Wright-Patterson AFB

2a. REPORT SECURITY CLASSIFICATION

Unclassified

2b. GROUP

3. REPORT TITLE

HEAT TRANSFER COEFFICIENTS FOR TWO-PHASE (WATER/AIR) FLOW OVER A TUBE BANK

4. DESCRIPTIVE NOTES (Type of report and inclusive dates)

Final Report

5. AUTHOR(S) (First name, middle initial, last name)

RAYMOND A. CARPENTER, 1Lt, USAF

6. REPORT DATE

May 72

7a. TOTAL NO. OF PAGES

70

7b. NO. OF REFS

14

8a. CONTRACT OR GRANT NO.

N/A

b. PROJECT NO.

GNE/PH/72-2

c.

d.

9a. ORIGINATOR'S REPORT NUMBER(S)

GNE/PH/72-2

9b. OTHER REPORT NO(S) (Any other numbers that may be assigned this report)

10. DISTRIBUTION STATEMENT

Distribution of this document is unlimited.

11. SUPPLEMENTARY NOTES

Approved for public release; IAW AFR 190-17

Keith A. Williams, 1st Lt., USAF
Acting Director of Information

12. SPONSORING MILITARY ACTIVITY

Aerospace Research Laboratory

13. ABSTRACT

Local heat and mass transfer coefficients were determined for a range of mass flux ratios and spray-water injection temperatures which included

0.060 to 0.167 at 125°F

0.069 to 0.250 at 140°F

0.058 to 0.253 at 150°F

0.060 to 0.203 at 160°F

The air Reynolds numbers during these tests were in the range 20,000 to 25,000. These Reynolds numbers were based on the minimum flow area within the tube bank and the tube outer diameter.

An average overall heat transfer coefficient of 13.88 Btu/hr-°F-ft was determined at a tubeside mass flow rate of 5491 lbm/hr and initial tubeside temperatures of 125°F and 140°F. The components of the overall heat transfer coefficient are reported for each case investigated.

A total heat transfer coefficient and heat transfer amplification factor are defined and reported as functions of mass flux ratio. The maximum amplification factor was 6.62 at an Air Reynolds number of 20,200 and mass flux ratio of 0.17.

La

LINK A

LINK B

LINK C

ROLE

WT

ROLE

WT

ROLE

W

Amplification Factor

IR

HEAT TRANSFER COEFFICIENTS
FOR TWO-PHASE (WATER/AIR)
FLOW OVER A TUBE BANK

THESIS

GNE/PH/72-2

Raymond A. Carpenter
1/Lt USAF

Distribution of this document is unlimited.

IC

HEAT TRANSFER COEFFICIENTS
FOR TWO-PHASE (WATER/AIR)
FLOW OVER A TUBE BANK

THESIS

Presented to the Faculty of the School of Engineering
of the Air Force Institute of Technology

Air University

in Partial Fulfillment of the
Requirements for the Degree of
Master of Science

by

Raymond A. Carpenter, B.S.

1/Lt

USAF

Graduate Nuclear Engineering

June 1972

Id

Preface

This study represents the first attempt to measure data with a new piece of equipment. Because of this, the design of the apparatus and the experimental procedure used have been discussed at length.

I would like to thank Dr. Elrod and Dr. Wright of the AFIT Aeromechanical Department for their continuing advice and assistance throughout the course of my work. I am also indebted to Mr. John Flahive, my laboratory assistant, for his efforts in constructing the experimental apparatus. My deepest appreciation to Dr. Ian Finlay, of the National Engineering Laboratory, Glasgow, Scotland for suggesting the problem while assigned to the Thermo-Mechanical Branch of the Aerospace Research Laboratory at Wright-Patterson Air Force Base, Ohio. A special thank you, to my wife, for her encouragement and for typing the thesis.

Raymond A. Carpenter

Contents

	Page
Preface	ii
List of Figures	v
List of Tables	vi
List of Symbols	vii
Abstract	x
I Introduction	1
Background	2
Purpose	4
Scope	4
II Apparatus	5
Tube Bank 1	5
Spray-Tube Design	8
Tube Bank 2	11
Air Supply	11
Water Supply	14
Calibration	15
Thermocouples	15
Strip Chart Recorders	17
Rotameters	17
III Theory	18
IV Experimental Procedure and Data Reduction	25
Local Heat Transfer Coefficients	25
Overall Heat Transfer Coefficients	28
Data Reduction	30
Air Mass Flow Rate	30
Tubeside Mass Flow Rate	30
Local Heat and Mass Transfer Coefficients	31
Total Heat Transfer Coefficients	32
Amplification Factor	33
Overall Heat Transfer Coefficients	34
V Results and Discussion	38
Overall Heat Transfer Coefficients	44
Total Heat Transfer Coefficients	44

Contents Continued

	Page
VI Conclusions	46
VII Recommendations for Further Study	48
Bibliography	51
Appendix I	53
Experimental Results in Tabular Form	53
Vita	60

List of Figures

Figure		Page
1	Schematic of Test Apparatus.	6
2	Thermocouple Instrumentation- Tube Bank 1	7
3	Spray-Tube Construction	9
4	Water Heating and Supply System	10
5	Thermocouple Instrumentation- Tube Bank 2	12
6	Heat Exchanger Instrumentation	13
7	Bank 2 Manifolds	16
8	Resistance Analog to Heat Transfer	19
9	Parameter Variation Within Tube Segment(dx)22	
10	140°F Survey Test Results.	39
11	150°F Survey Test Results.	40
12	160°F Survey Test Results.	41
13	Constant Air Mass Flow Rate Heat Transfer Coefficients	43
14	Triangular Tube Bank	48

List of Tables

Table		Page
1	Survey Test Parameter Range	54
2	Constant Air Mass Flow Rate Test. Parameter Range	55
3	Local Coefficients for Survey Tests . . .	56
4	Local Coefficients for Constant Air . . . Mass Flow Rate	57
5	Overall Heat Transfer Coefficient Components	58
6	Total Heat Transfer Coefficients and. . . Amplification Factors	59

List of Symbols

Symbol	Definition	Units
A	Shellside heat transfer area	ft^2
A _F	Heat transfer amplification factor	dimensionless
A _{TOT}	Total heat transfer area	ft^2
β	Local evaporative mass transfer coefficient	$\text{Btu/hr-ft}^2\text{-}^\circ\text{F}$
C _A	Air heat capacity	$\text{Btu/lbm-}^\circ\text{F}$
C _L	Water heat capacity	$\text{Btu/lbm-}^\circ\text{F}$
C _V	Water vapor heat capacity	$\text{Btu/lbm-}^\circ\text{F}$
H _{Aj}	Air enthalpy at state j	Btu/lbm
H _A	Convective heat transfer coefficient between air and tube wall	$\text{Btu/hr-ft}^2\text{-}^\circ\text{F}$
H _L	Effective convective heat transfer coefficient across shellside liquid	$\text{Btu/hr-ft}^2\text{-}^\circ\text{F}$
H _{LA}	Local coefficient between air and shellside flow	$\text{Btu/hr-ft}^2\text{-}^\circ\text{F}$
H _{LT}	Convective heat transfer coefficient between tube-side flow and tube wall	$\text{Btu/hr-ft}^2\text{-}^\circ\text{F}$
H _{TL}	Convective heat transfer coefficient between tube wall and shellside flow	$\text{Btu/hr-ft}^2\text{-}^\circ\text{F}$
H _{TOT}	Total heat transfer coefficient based on total heat transferred, total area, and total average temperature difference	$\text{Btu/hr-ft}^2\text{-}^\circ\text{F}$
H _W	Effective convective heat transfer coefficient across tube wall	$\text{Btu/hr-ft}^2\text{-}^\circ\text{F}$

List of Symbols Continued

Symbol	Definition	Units
ID	Tube inner diameter	ft
K_A	Air thermal conductivity	Btu/hr-ft ² -°F
K_L	Water thermal conductivity	Btu/hr-ft ² -°F
K_W	Wall thermal conductivity	Btu/hr-ft ² -°F
l	Length of shellside heat transfer area	ft
L	Water latent heat of vaporization	Btu/lbm
Nu	Nusselt number based on local convective heat transfer coefficient and tube diameter	dimensionless
OD	Tube outer diameter	ft
PB	Barometric pressure	psia
Pr	Prandtl number	dimensionless
PST	Water vapor saturation pressure	psi
PV	Partial pressure of water vapor	psi
Q_i	Heat flux across i th resistance	Btu/hr-ft ²
Q_{TOT}	Total heat flow rate across heat exchanger	Btu/hr
Re_A	Air Reynolds number based on minimum flow area within tube bank and tube outer diameter	dimensionless
Re_L	Shellside water Reynolds number based on tube outer diameter	dimensionless

List of Symbols Continued

Symbol	Definition	Units
Re_T	Tubeside water Reynolds number based on tube inner diameter	dimensionless
R_i	Heat transfer resistance across i th resistance	$ft^2-^{\circ}F-hr/Btu$
r_i	Tube inner radius	ft
r_o	Tube outer radius	ft
r_{iw}	Tube outer radius	ft
r_{ow}	Radius from tube center to outer surface of shellside flow	ft
Sc	Schmidt number	dimensionless
Sh	Scherwood number	dimensionless
t_A	Air dry bulb temperature	$^{\circ}F$
ΔT_{ave}	Overall temperature difference between average air and average tubeside temperatures	$^{\circ}F$
T_o	Initial tubeside temperature	$^{\circ}F$
$\Delta T_{overall}$	Overall temperature difference between tube-side flow and spray	$^{\circ}F$
W_A	Air mass flow rate	lbm/hr
W_e	Evaporative mass flow rate	lbm/hr
W_L	Spray-water mass flow rate	lbm/hr
W_T	Tubeside mass flow rate	lbm/hr

Abstract

Local heat and mass transfer coefficients were determined for a range of mass flux ratios and spray-water injection temperatures which included

0.060 to 0.167 at 125°F

0.069 to 0.250 at 140°F

0.058 to 0.253 at 150°F

0.060 to 0.203 at 160°F

The air Reynolds numbers during these tests were in the range 20,000 to 25,000. These Reynolds numbers were based on the minimum flow area within the tube bank and the tube outer diameter.

An average overall heat transfer coefficient of 13.88 Btu/hr-°F-ft² was determined at a tubeside mass flow rate of 5491 lbm/hr and initial tubeside temperatures of 125°F and 140°F. The components of the overall heat transfer coefficient are reported for each case investigated.

A total heat transfer coefficient and heat transfer amplification factor are defined and reported as functions of mass flux ratio. The maximum amplification factor was 6.62 at an air Reynolds number of 20,200 and mass flux ratio of 0.17.

HEAT TRANSFER COEFFICIENTS
FOR TWO-PHASE (WATER/AIR)
FLOW OVER A TUBE BANK

I. Introduction

Spray-flow may be defined as that flow situation which exists when a rapidly flowing gas entrains and carries with it dispersed liquid droplets. In any tube bank, spray-flow exists only over the first few rows of tubes. From that point on the two-phase flow becomes nonuniform in character, the liquid flowing in sheets or slugs as compared to droplets. The droplet model is, however, the most readily described from a theoretical standpoint and will be used throughout the study.

The theoretical description of air/water spray-flow heat transfer is a more complicated task than that encountered in single-phase heat transfer. With spray-flow, a water film forms on heat transfer surfaces and convective heat and mass transfer takes place between the liquid film and the two-phase free stream flow. In order to compute the overall resistance to heat transfer for a specific situation, as in spray-flow through a heated tube bank, both an evaporative mass transfer coefficient and the following heat transfer coefficients must be known:

1. The convective heat transfer coefficient

between the flow within the tubes (the tubeside flow) and the tube wall, H_{LT} .

2. Thermal conductivity across the tube wall, K_W .

3. The convective heat transfer coefficient between the outer tube surface and the liquid film flowing on that surface (the shellside flow), H_{TL} .

4. Thermal conductivity across the shellside liquid film, K_L .

5. The convective heat transfer coefficient between the surface liquid and the free stream two-phase flow, H_{LA} .

If the liquid film which covers the tubes of the heat exchanger is assumed to be thin and well mixed there will be no temperature gradients within the film. The heat transfer resistance across this film may then be neglected. The film can be considered a separate source of thermal energy and only two resistances to heat transfer need be considered; an overall resistance composed of the sum of the first three components, and the local resistance contributed by the fifth component.

Background

Interest in spray-flow heat transfer was first generated some ten years ago as a result of an investigation by Elperin (Ref. 4). Elperin reported increased heat transfer over a tube bank when water spray was

introduced into the cooling air stream. The increases reported were as much as 30 times the heat transfer normally available with single-phase air heat exchangers, and the pressure losses through the heat exchanger were not significantly greater in two-phase flow as compared to single-phase gas flow. Unfortunately, the data reported were not complete.

Since that time a number of investigations have been carried out to more clearly define and delineate the mechanisms involved in spray-flow heat transfer. Acrivos, et al, (Ref. 1) proposed four different models of a spray-flow system and carried out comparative analytical and experimental analysis of each model. Hoelscher (Ref. 8) extended the work of Acrivos and measured the variation of the overall heat transfer coefficient with angular position around a circular cylinder. Takahara (Ref. 14) extended Hoelscher's work and as pointed out by Hodgson, et al, (Ref. 7) more carefully established the temperature difference (and heat transfer coefficient) between the cylinder wall and the free stream flow.

Finlay, et al, (Ref. 5) performed experiments to measure the overall heat transfer coefficients for air/water spray-flows in a tube bank. He utilized an energy balance to develop a set of differential equations which were used to predict the performance of spray-flow heat

exchangers. He did not, however, measure the local heat and mass transfer coefficients but was forced by the lack of experimental data to assume values for these coefficients.

Purpose

Finlay (Ref. 6) proposed a method of experimentally determining the local convective heat and mass transfer coefficients as well as the overall heat transfer coefficients. The purpose of this study was to use the proposed method to determine experimentally these coefficients and the corresponding overall heat transfer coefficients.

Scope

The objectives of this study included the following:

1. To complete the design and construction of a spray-flow heat exchanger as proposed by Finlay (Ref. 6).
2. To determine local heat and mass transfer coefficients within ranges of spray-water/air mass flux ratios from 0.05 to 0.15, and spray-water injection temperatures from 125°F to 160°F.
3. To determine overall heat transfer coefficients between the tubeside flow and shellside flow.
4. To determine total heat transfer coefficients which include the local heat and mass transfer coefficients.

II. Apparatus

A major part of the effort of this study was devoted to the final design and construction of a test device which would permit an in depth investigation of spray-flow heat transfer. The basic design followed was initiated by Finlay (Ref. 6) for the Aerospace Research Laboratory (ARL). A schematic diagram of the apparatus is shown in Figure 1.

The heat exchanger contained two banks of tubes. Each bank consisted of 70 1/4 inch O.D. copper tubes, arranged in a 1.5xO.D. equilateral pitching, with 10 rows of tubes, 7 tubes per row.

Tube Bank 1

Tube bank 1 (Figure 2) was an adiabatic bank used to generate the spray-flow and determine the local heat and mass transfer coefficients. Nine of the tubes in Bank 1 contained copper-constantan thermocouples located at the forward stagnation point. These were mounted flush with the outer tube surface and insulated from the tube wall. This configuration was used to insure that the thermocouples measured only the temperature of the shellside liquid. Three additional tubes at the bottom of Bank 1 were instrumented with thermocouples. These were U-shaped catcher tubes which were exposed to the exit two-phase spray and were expected to read the adiabatic saturation temperature.

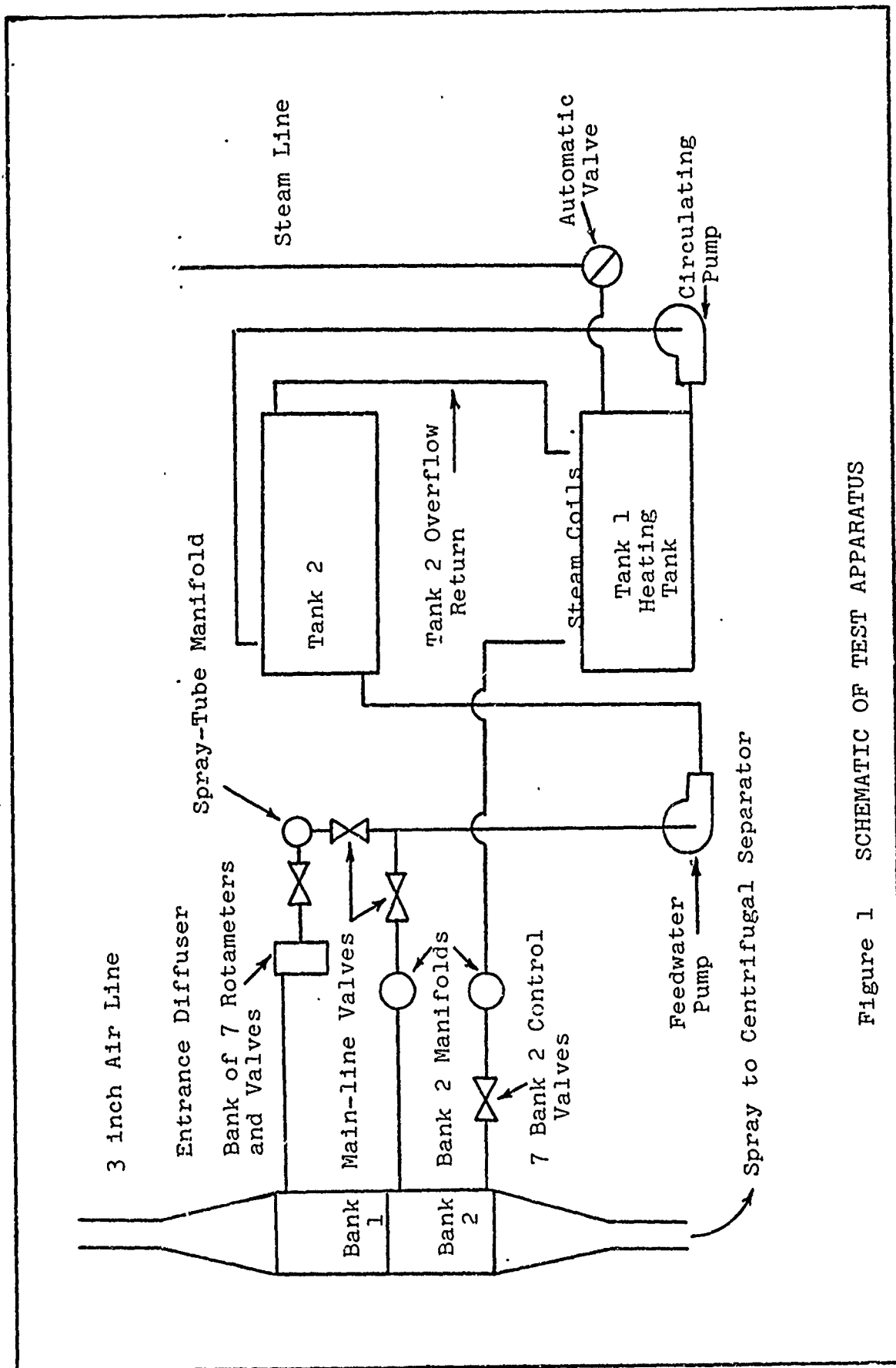
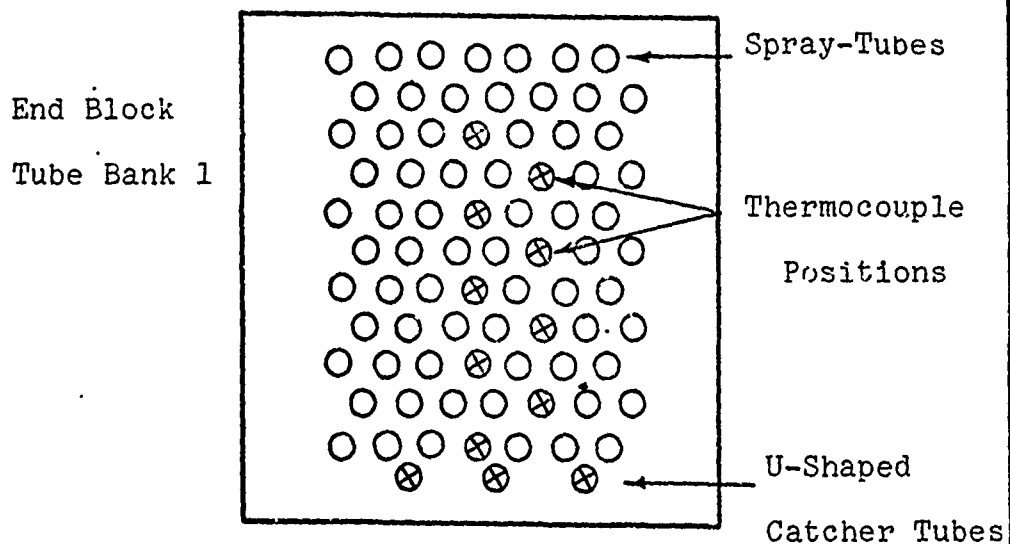


Figure 1 SCHEMATIC OF TEST APPARATUS



Section Through Instrumented Tube

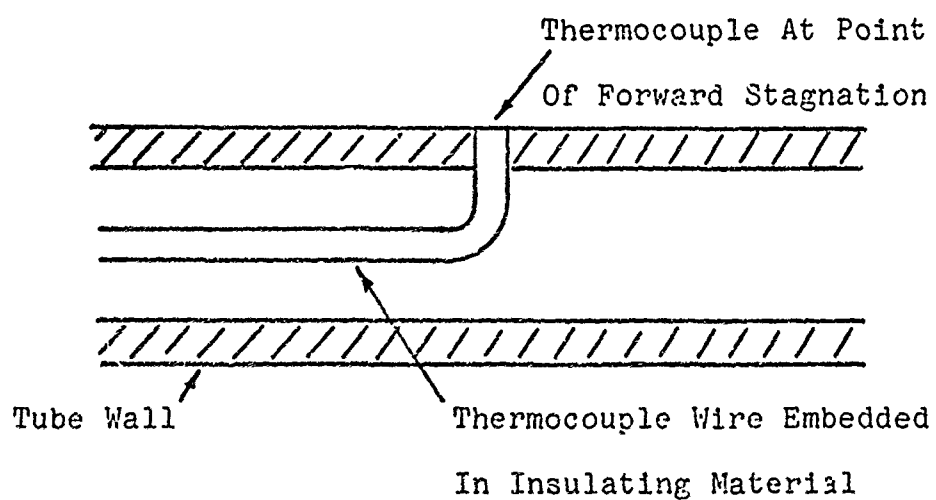


Figure 2 THERMOCOUPLE INSTRUMENTATION -

TUBE BANK 1

Spray-Tube Design

The first tube row in tube bank 1 contained seven spray tubes. The design of these tubes is shown in Figure 3. The spray-water mass flow rate in each spray tube was monitored and controlled through a bank of seven Brooks Full-View Rotameters, shown in Figure 4.

The spray-tubes were constructed of heavy-wall, half-hard, brass tubing. Each tube was 18 inches long and 0.250 inches in diameter. A six inch section of each tube was milled down to 0.225 inches and a 6 X 0.020 X 0.027 inch rectangular groove cut into the tube wall within the milled section. Evenly spaced holes 0.031 inches in diameter were then drilled through the tube wall within the groove. The entire milled section was then covered with a closely woven Nylon cloth of uniform porosity.

Water flowing in the spray-tubes was forced into small holes in the tube wall, through the Nylon cloth, and was entrained in the air stream. This process is shown in Figure 3 by arrows. This method of water injection was used since it allowed for the measurement of spray-water input temperatures and was designed to create a more uniform distribution of spray liquid within the tube bank than could have been achieved with spray-nozzles. However, the design of the tube bank made it

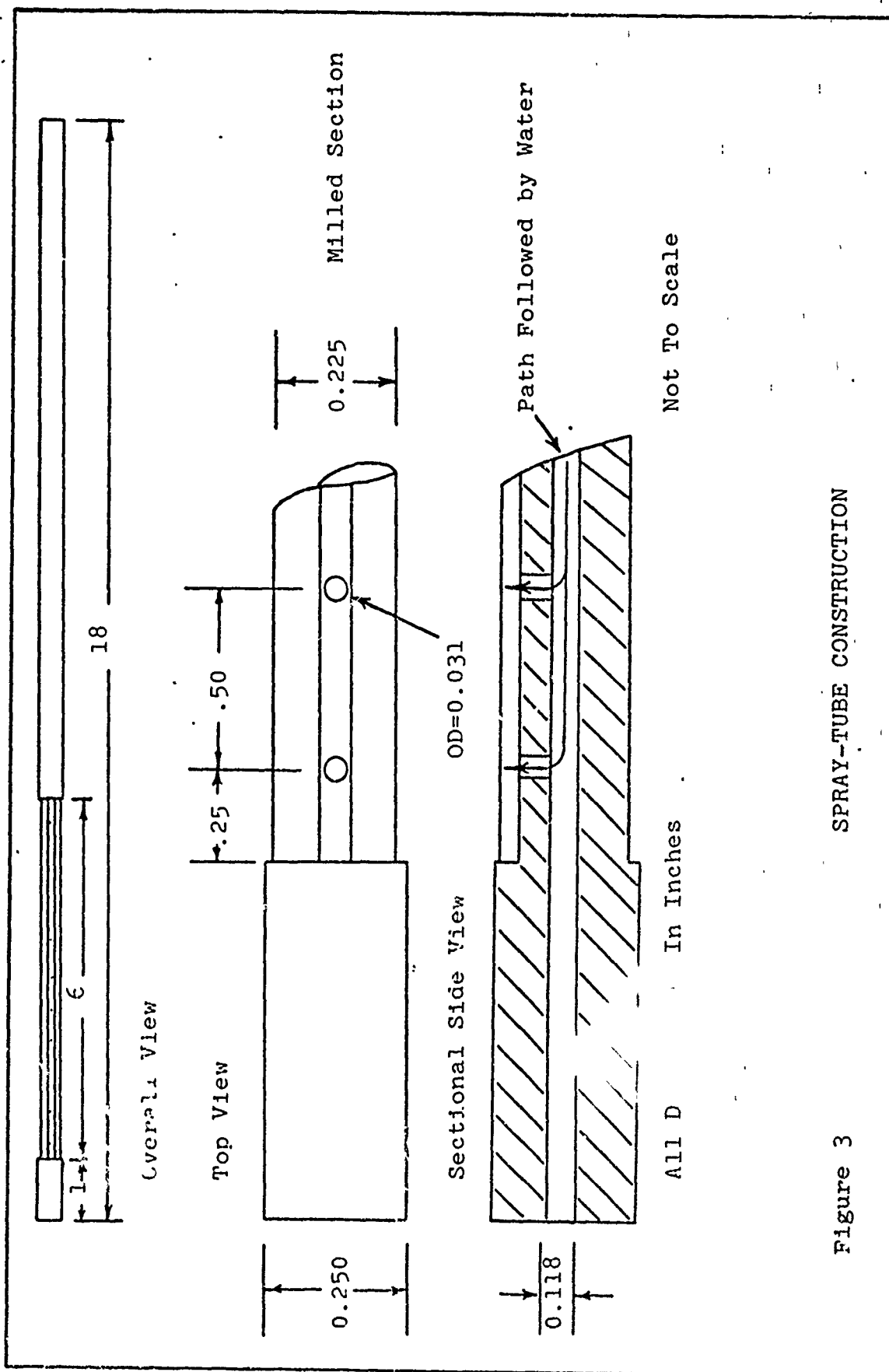
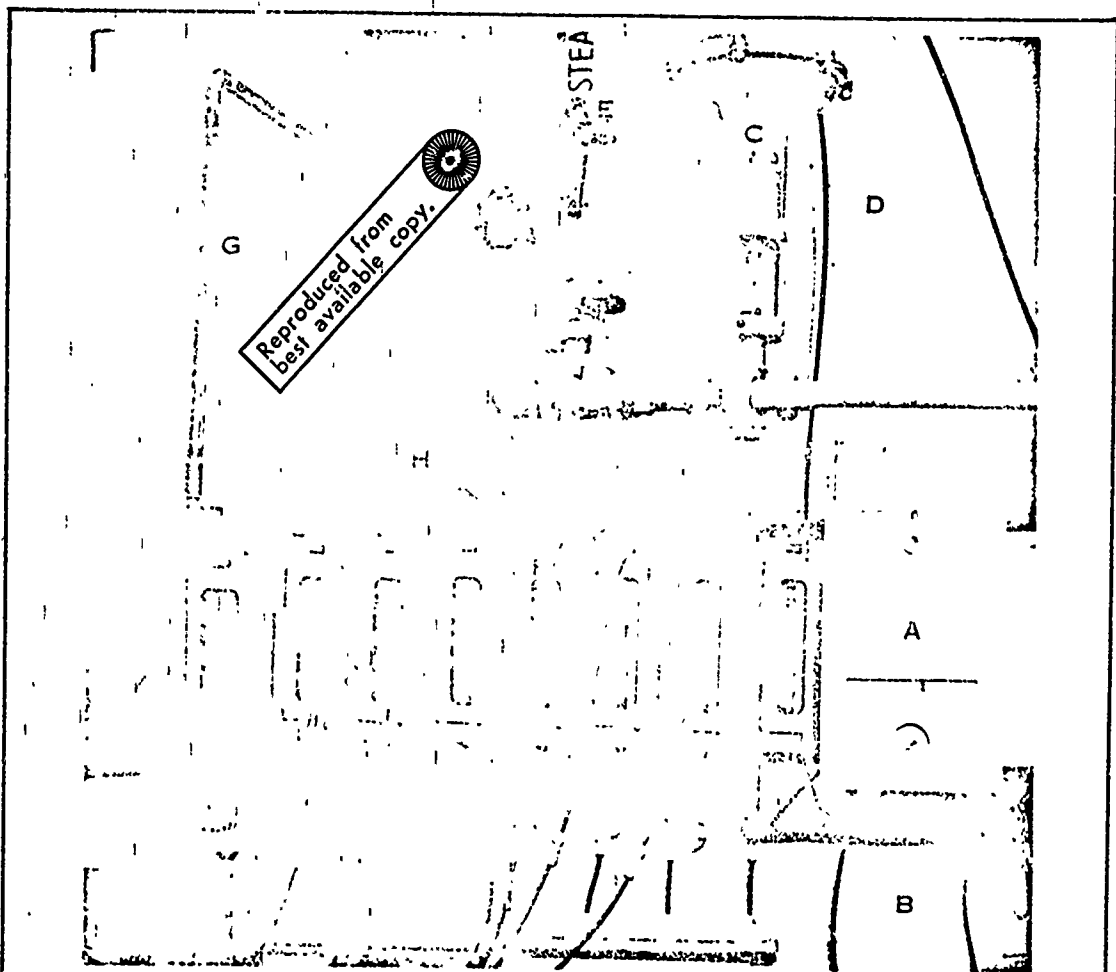


Figure 3 SPRAY-TUBE CONSTRUCTION



- A = Temperature Control Unit
- B = Tank 1
- C = Automatic Steam Control Valve
- D = Tank 2
- E = Steam Line
- F = Spray-Tube Rotameters
- G = Tank 1/Tank 2 Circulation Line
- H = Air Exhaust From Centrifugal Separator

Figure 4 WATER HEATING AND SUPPLY SYSTEM

impossible to verify, by direct observation, that the spray was uniform within the tube bank.

Tube Bank 2

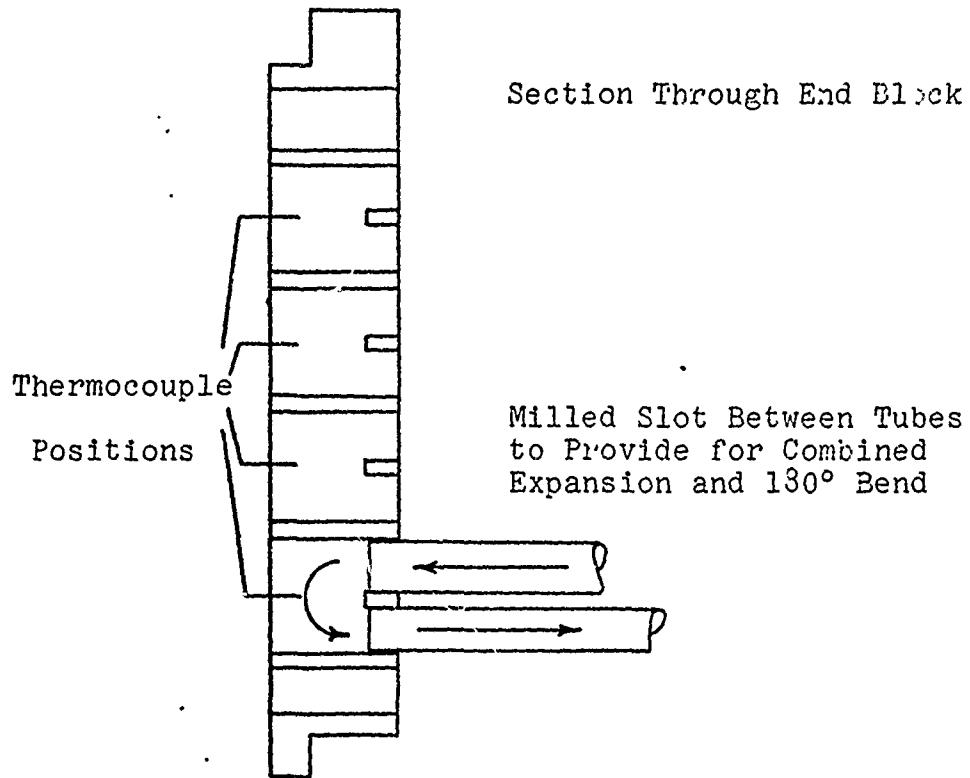
Bank 2 was heated by a tubeside flow of water which was assumed to be turbulent. The water flowing in bank 2 was cooled by the air/water spray emerging from bank 1. Twenty tubes in bank 2 were instrumented with thermocouples. These were located at inlet to the tubes immediately following the 180° bend, which also provided a slight deacceleration of the fluid, shown in Figure 5. In this configuration, the tubeside flow was subjected to a strong mixing action. The upper section of bank 1 and the lower section of bank 2 were supplied with access holes to permit the measurement of pressure within the banks and the air wet- and dry-bulb temperatures. The thermocouple installations of tube bank 1 and 2 are shown in Figure 6.

Air Supply

Air was supplied to the heat exchanger from the laboratory supply. The air was delivered through a 3 inch O.D. line, passed through a 1 inch bore orifice meter fitted with flange taps, and controlled by a large valve. The heat exchanger was connected to the air line through an aluminum diffuser. This diffuser was

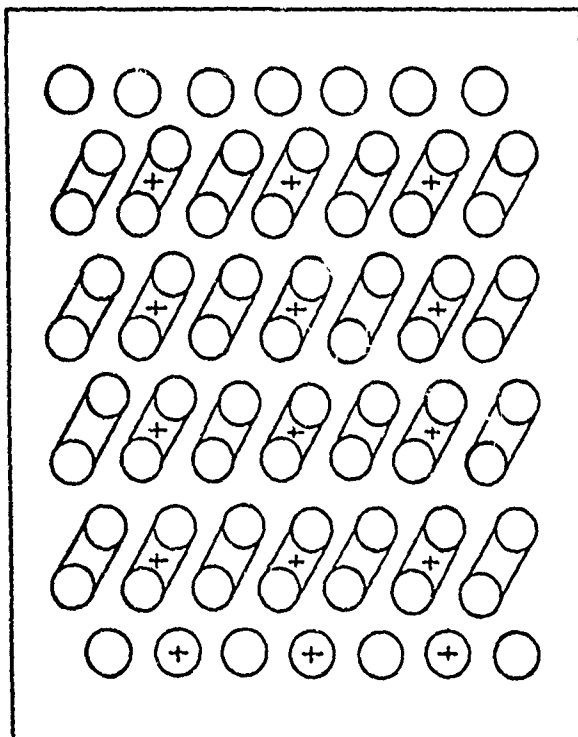
Figure 5 THERMOCOUPLE INSTRUMENTATION -

TUBE BANK 2



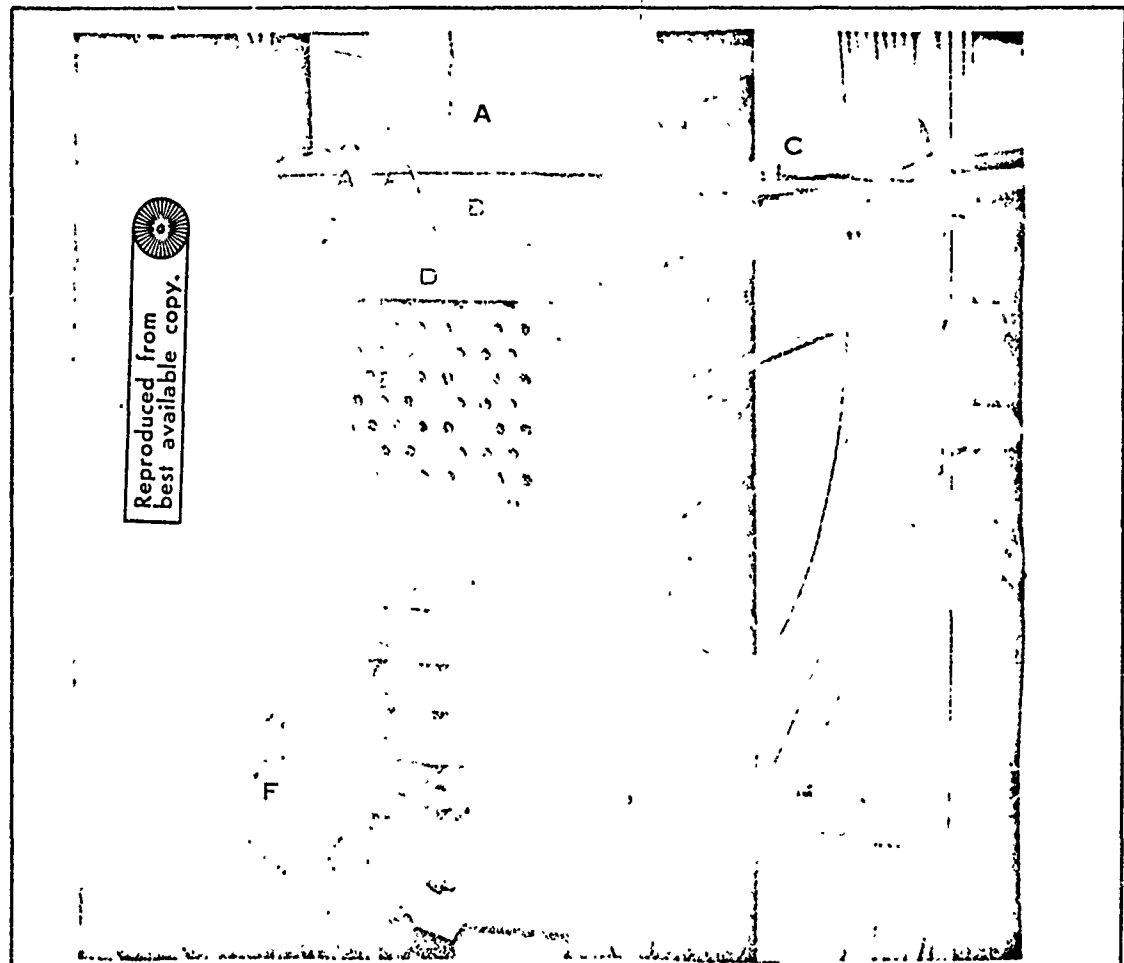
End Block
Bank 2

Milled
Slots
Between
Tubes



Thermocouple
Positions

Catcher Tubes



- A = Air Entrance Diffuser
- B = Pressure Tap for Stagnation Pressure
- C = Air Wet- and Dry-Bulb Thermometer Access Ports
- D = Spray-Tube Location in Bank 1
- E = Bank 1 Thermocouple Locations
- F = Bank 2 Thermocouple Locations

Figure 6 HEAT EXCHANGER INSTRUMENTATION

instrumented with a thermocouple to monitor the air input temperature. An identical arrangement at the outlet directed the water/air spray into a centrifugal separator. The separator exhausted air to the atmosphere and was periodically pumped to return water to the heating system.

Water Supply

Two large open tanks were employed in the water supply system. A lower tank (tank 1) contained coils of copper tubing through which steam at 100 psi was fed to heat the water. The upper tank (tank 2) contained a heat sensing element as part of a Powers Series 200 Temperature Controller which was used to control the steam flow through a pneumatic valve.

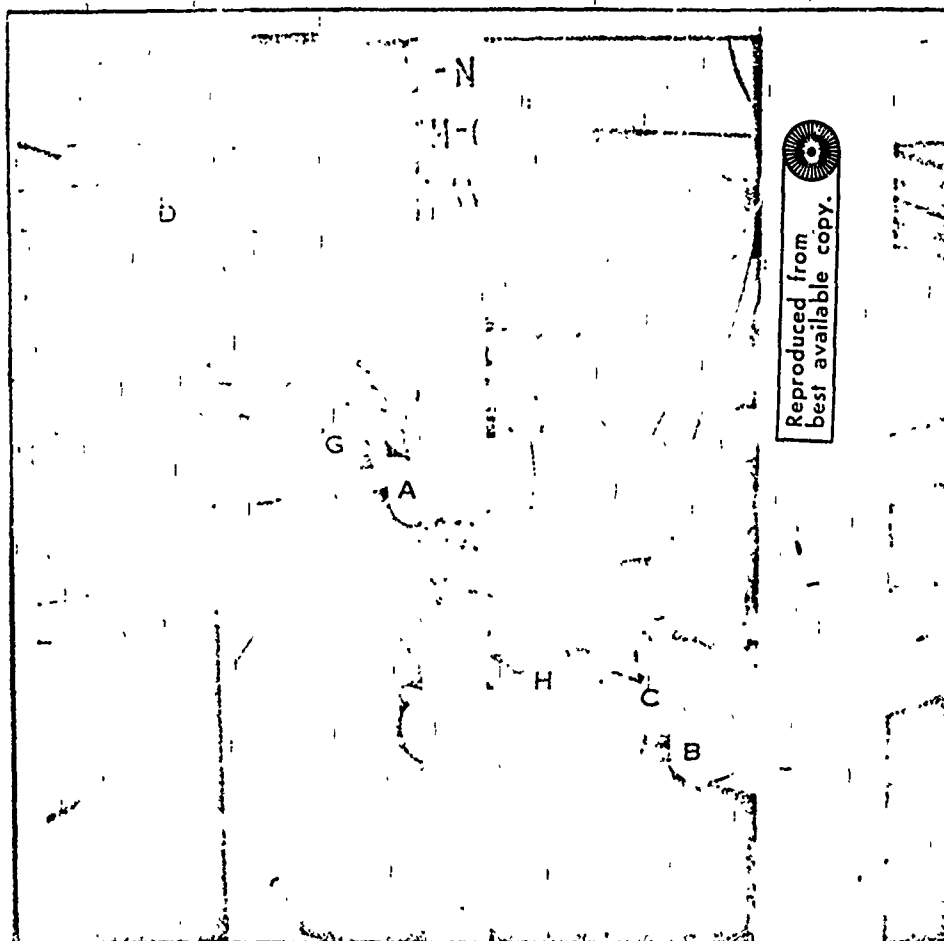
The water supply system incorporated three TEEL Close-Coupled Centrifugal Pumps. These were used to circulate heated water through the storage tanks (Pump A), to pump heated feedwater to the spray-tube and bank 2 inlet manifolds (Pump B), and to periodically drain the centrifugal separator into tank 1 (Pump C).

Feedwater for both the spray-tubes and the tube-side flow of bank 2 was obtained from the upper tank. A valve arrangement allowed the water from this single tank to be pumped to the inlet manifolds for either

the spray-tubes or bank 2 or both. Each tube in bank 2 was provided with manometer taps to provide pressure measurements which could be used to measure the flow into and out of the tube bank, shown in Figure 7. In addition, each tube was provided with a valve to regulate the tubeside flow and insure equal flowrates in each tube. The cooled tubeside flow was collected in a return manifold and passed into tank 1 for re-heating. Spray water was collected in a centrifugal separator and periodically returned to tank 1. Figure 7 shows the feed and return manifolds for bank 2.

Calibration

Thermocouples. The thermocouples were prepared by the AFIT shops from the same spool of copper and constantan wire. Ten of these were tested at the University of Minnesota Department of Mechanical Engineering. For average temperatures of 88.656°C and 99.255°C the individual thermocouple voltages, measured with a Wenner potentiometer, were within one microvolt of the average sample. The average voltages for both temperatures were found to be 0.55% higher than the values in the National Bureau of Standards publication No. 590. The other thermocouples used were assumed to exhibit the same characteristics as the thermocouples tested.



- A = Bank 2 Feed Manifold
- B = Bank 2 Return Manifold
- C = Bank 2 Control Valve
- D = Spray-Tubes
- E = Bank 2 Feed Tubes
- F = Bank 2 Return Tubes
- G = Entrance Manometer Taps
- H = Return Manometer Taps

Figure 7 BANK 2 MANIFOLDS

Strip Chart Recorders. The thermocouple voltages were recorded on Honeywell Electronik 16 Multipoint Strip Chart Recorders. These were calibrated in Millivolts before each test run with a Honeywell potentiometer. If thermocouple output exceeded the selected millivolt range during any specific test, the recorders were recalibrated over a range sufficient to include all data.

Rotameters. The rotameters were designed to measure flow rates for fluids of specific gravity = 1. In the temperature range of interest (125° F to 160° F) water has specific gravity of 0.9871 to 0.9718. The meters were tested at a fluid temperature of 140° F and meter settings found which would correctly measure flow rates of 20, 30, 40, 50, and 60 lbm/hr. This group was later expanded to include 27.22 and 33.63 lbm/hr. Calculations showed that over the temperature range of interest these same settings could be used with less than 2% error.

III. Theory

When a two-phase mixture flows through a heated tubebank, thermal energy is transferred from the tube-side flow, through the tubewall, and causes conductive heating of the shellside liquid. Convective heat transfer then occurs between the shellside liquid and the free-stream air.

By employing the electrical analog of heat transfer, (Ref. 9) five components of resistance may be defined across $(T_o - t_A)$, the temperature gradient between the tubeside bulk temperature and the air dry-bulb temperature. These five resistances are diagrammed in Figure 8.

If steady-state heat transfer is assumed and evaporation ignored, then the amount of heat transferred across each resistance is equal to that transferred across any other resistance. That is:

$$q_1 = q_2 = q_3 = q_4 = q_5 = q \quad (3-1)$$

where

$$q_1 = h_{LW} 2\pi r_i l (T_1 - T_2) \quad (3-2)$$

$$q_2 = \frac{K_W 2\pi l (T_2 - T_3)}{\ln(r_o/r_i)} \quad (3-3)$$

$$q_3 = h_{WL} 2\pi r_o l (T_3 - T_4) \quad (3-4)$$

$$q_4 = \frac{K_L 2\pi l (T_4 - T_5)}{\ln(r_{ow}/r_{iw})} \quad (3-5)$$

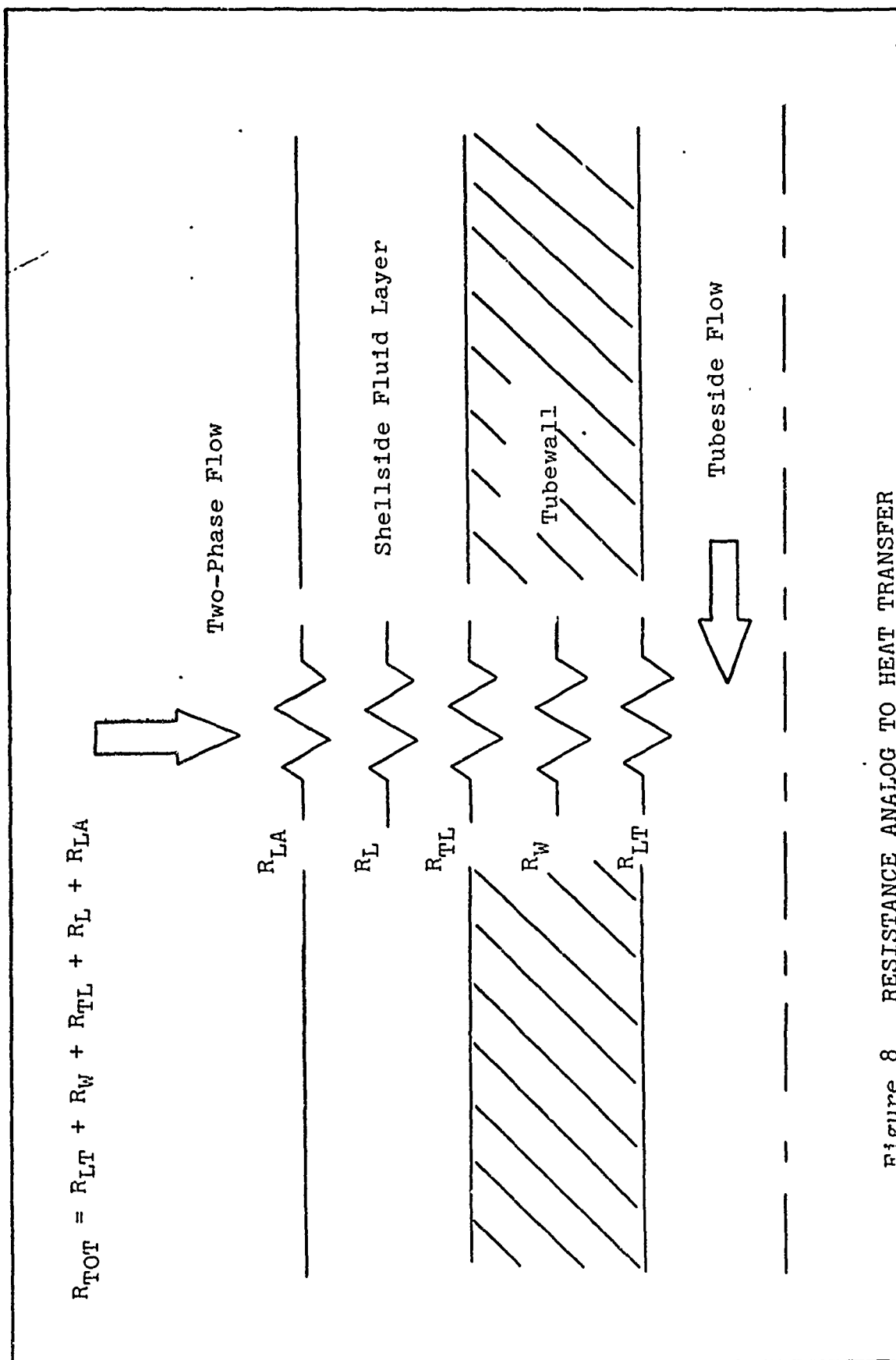


Figure 8 RESISTANCE ANALOG TO HEAT TRANSFER

$$q_5 = h_{LA} 2\pi r_{ow} l (T_5 - T_6) \quad (3-6)$$

Furthermore, equations may be written defining the heat flux per unit area based on the tube outer diameter.

$$Q_1 = \frac{q_1}{A} = \frac{h_{LW} 2\pi r_{i1} l (T_1 - T_2)}{2\pi r_o l} = H_{LW} (T_1 - T_2) \quad (3-7)$$

$$Q_2 = \frac{q_2}{A} = \frac{K_W 2\pi l (T_2 - T_3)}{2\pi r_o l (\ln(r_o/r_{i1}))} = H_W (T_2 - T_3) \quad (3-7)$$

$$Q_3 = \frac{q_3}{A} = \frac{h_{WL} 2\pi r_o l (T_3 - T_4)}{2\pi r_o l} = H_{WL} (T_3 - T_4) \quad (3-9)$$

$$Q_4 = \frac{q_4}{A} = \frac{K_L 2\pi l (T_4 - T_5)}{2\pi r_o l (\ln(r_{ow}/r_{iw}))} = H_L (T_4 - T_5) \quad (3-10)$$

$$Q_5 = \frac{q_5}{A} = \frac{h_{LA} 2\pi r_{ow} l (T_5 - T_6)}{2\pi r_o l} = H_{LA} (T_5 - T_6) \quad (3-11)$$

These five equations may be solved simultaneously and combined into one overall equation:

$$\frac{q}{A} = \frac{\Delta T_{overall}}{\frac{1}{H_{LT}} + \frac{1}{H_W} + \frac{1}{H_{TL}} + \frac{1}{H_L} + \frac{1}{H_{LA}}} \quad (3-12)$$

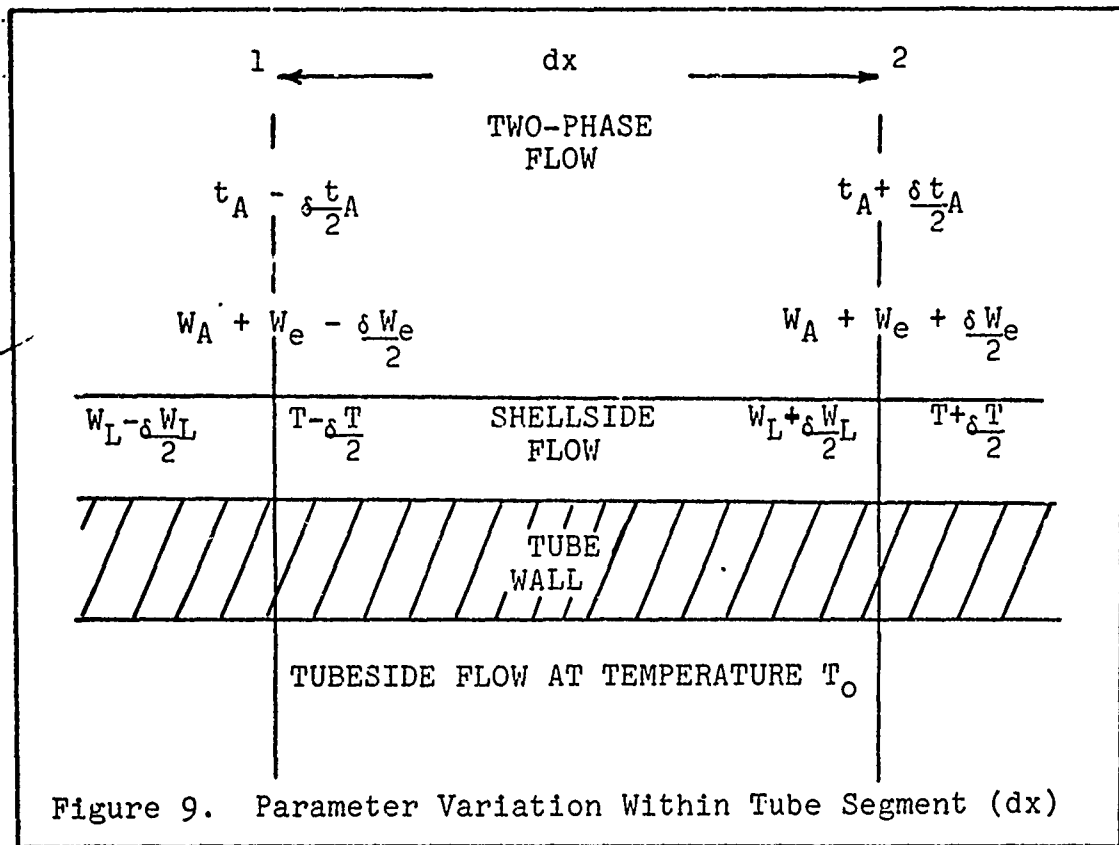
where the denominator is the overall resistance to heat transfer and is equal to the reciprocal of the overall heat transfer coefficient. If the assumption is now made that $T_4 = T_5$, that is, no temperature gradients exist within the shellside liquid, then Q_4 , the heat flux across the shellside liquid, is zero. Equations (3-7), (3-8), and (3-9) can be combined in an overall heat transfer coefficient. This coefficient

is given by:

$$\frac{1}{U} = \frac{1}{H_{LT}} + \frac{1}{H_W} + \frac{1}{H_{TL}} \quad (3-13)$$

The convective heat transfer coefficient at the air/water interface, H_{LA} , then becomes a local heat transfer coefficient which can be determined separately from the overall coefficient, U .

Convective heat transfer from the hot shellside liquid to the free-stream air results in an increase in the air dry-bulb temperature and a corresponding decrease in the temperature of the shellside fluid. Simultaneously, evaporative mass transfer from the shellside film to the air results in an increase of the partial pressure of water vapor in the air, a reduction in the mass flow rate of the liquid phase, and a further lowering of the liquid phase temperature. Hence, four parameters, the air dry-bulb temperature (t_A), the partial pressure of the water vapor (PV), the spray water temperature (T), and the spray water mass flow rate (W_L) change simultaneously with respect to the shellside area (A). The changes in these parameters, over a small section of the total area for heat transfer is shown schematically in Figure 9.



The changes in these parameters can be described by four simultaneous differential equations developed by Finlay, et al, (Ref. 5). Finlay assumed that each tube in the tube bank could be divided into N sections of width dx . Each such section was assumed to contain tubeside fluid at a single bulk temperature, T_0 . The shellside fluid was assumed well mixed and heat and mass transfer was considered to take place only while the fluid was flowing on the tube surface. Further, the heat and mass transfer coefficients at the air/water interface were assumed to be described by relations of the form:

$$Nu = f(Re^n, Pr^m) \quad (3-14)$$

$$Sh = f(Re^n, Sc^m) \quad (3-15)$$

These relations were used to define an evaporative mass transfer coefficient in terms of the heat transfer coefficient in the following manner:

For equal Reynolds numbers, the ratio of (3-14) to (3-15) is:

$$\frac{Nu}{Sh} = \frac{Pr}{Sc}^m \quad (3-16)$$

For air/water vapor system, $Pr/Sc = 1$

Hence:

$$Nu = Sh \quad (3-17)$$

But

$$Nu = \frac{H_{LA} d}{K} \quad (3-18)$$

$$Sh = \frac{\beta d}{D_P} \quad (3-19)$$

Therefore, the mass transfer coefficient is related to the convective heat transfer coefficient by:

$$\beta = \frac{D_P}{K} H_{LA} \quad (3-20)$$

The differential equations developed by Finlay are:

$$\frac{dt_A}{dA} = \frac{H_{LA}(T - t_A)}{W_A C_A} [1 + \frac{C_V \beta (PST - PV)}{H_{LA}}] \quad (3-21)$$

$$\frac{dPV}{dA} = \frac{\beta}{0.622 W_A} \frac{(PB - PV)^2 (PST - PV)}{PB} \quad (3-22)$$

$$\frac{dT}{dA} = U \frac{(T_o - T)}{W_L C_L} - H_{LA} \frac{(T - t_A)}{W_L C_L} - L\beta \frac{(PST - PV)}{W_L C_L} \quad (3-23)$$

$$\frac{dW_L}{dA} = -\beta(PST-PV) \quad (3-24)$$

When spray-flow occurs across an adiabatic tube bank,

$(T_o - T) = 0$ and the equations become:

$$\frac{dt_A}{dA} = H_{LA} \frac{(T - t_A)}{W_A C_A} \left[1 + \frac{C_V \beta (PST-PV)}{H_{LA}} \right] \quad (3-25)$$

$$\frac{dPV}{dA} = \frac{\beta}{0.622 W_A} \frac{(P_B - PV)^2}{P_B} (PST-PV) \quad (3-26)$$

$$\frac{dT}{dA} = -H_{LA} \frac{(T - t_A)}{W_L C_L} - L\beta \frac{(PST-PV)}{W_L C_L} \quad (3-27)$$

$$\frac{dW_L}{dA} = -\beta(PST-PV) \quad (3-28)$$

If the temperature history of the spray water across an adiabatic bank is known, equations (3-25) - (3-28) can be integrated numerically to yield values of H_{LA} and β .

The overall heat transfer coefficients can be determined through the use of empirical relations for each of its component parts. Total heat transfer coefficients are determined by macroscopic energy balances over entrance and exit conditions. The calculational procedures used are outlined in Chapter IV.

IV. Experimental Procedure and Data Reduction

Before measurement of heat transfer data began, a series of initial tests of the experimental apparatus were completed. During these tests the orifice plate pressure drops associated with selected air mass flow rates were determined. In addition to the air flow tests, water was circulated through both the spray-tubes and the tubes of bank 2. This was done to check for leaks in the system and to allow time for the rapid initial formation of scale to occur on the clean tubes. Thermocouple connections were also tested and the entire system examined to determine if provisions had been made for the collection of all necessary data.

Local Heat Transfer Coefficients

On the basis of experimental procedure, the tests to determine local heat and mass transfer coefficients were divided into two categories.

1. A survey test sequence where the selected spray-water mass flow rates were held constant and air mass flow rates varied.

2. A constant air mass flow rate test sequence where the air mass flow rates were held constant and spray-water mass flow rates varied.

In the former series three spray-water injection temperatures were used, in the latter, two temperatures. The parameter range used in each series are shown in Tables 1 and 2, Appendix I. The same basic experimental procedure was used in each test.

For any particular test run, the desired water temperature was set on the Powers Series 200 Automatic Temperature Control and Pump A started to circulate water through tanks 1 and 2. Water was heated by the steam coils in tank 1 and pumped into tank 2. This circulation of water through the system was continued until the entire water storage system was at the desired temperature.

While the water was being heated, air flow through the heat exchanger was started at a level sufficient to produce the predetermined air mass flow rate. Air flow was continued for at least a half-hour to allow for the stabilization of the air wet- and dry-bulb temperatures. At this point the values of the air pressure upstream from the orifice plate, the pressure drop across the orifice plate, the barometric pressure, ambient temperature, and air dry- and wet-bulb temperatures were recorded. The first five of these variables were used in an approximate calculation of the air mass flow rate. If any great discrepancy (more than 10%) was involved between the desired value and the calculated value, adjustment of the air mass flow rate was made. Throughout

the course of the experiment any changes in the values of these parameters were noted. The air dry-bulb temperature was recorded continuously.

For the purpose of calculating a partial pressure of water vapor (PV) in the air, however, the initial air wet-and dry-bulb temperatures were assumed constant throughout any specific series of tests. Once the air flow had stabilized, these values were measured and used to determine PV from a psychometric chart (Ref. 10 page 435). This procedure was dictated by the fact that once spray had been introduced into the heat exchanger, vapor pressure could no longer be determined accurately. The access ports for the wet-and dry-bulb thermometers were positioned near the spray-tubes and the thermometers read spray-water temperatures.

With air flowing at the predetermined rate, water was supplied to the spray-tube manifold which fed seven individually monitored flow meters. These meters were monitored continuously until thermal equilibrium between the meters and the hot liquid flowing within them was achieved. This period, usually a half-hour, also allowed time for the individual tubes of bank 1 to become wetted with fluid. Throughout the course of the experiment spray-water temperature was monitored at the flow meters.

The Honeywell recorder was then calibrated in millivolts with a Honeywell potentiometer. Data were then

recorded for a short period of time to determine if all necessary thermocouples were operating properly, the reference junctions of the thermocouples were maintained at 32° F.

The two-phase flow was then allowed to stabilize. The temperature history of the shellside fluid during its passage through the adiabatic bank was recorded at random time intervals. Stabilization was considered to have occurred when visual comparison of the temperature profiles (temperature verses heat transfer area) indicated similarity. At this point the recorder was operated for an extended period. At the completion of the final observation, the necessary parameter changes were made depending on the test sequence and the above procedure repeated.

Overall Heat Transfer Coefficients

Measurements necessary for the computation of overall heat transfer coefficients were taken during the constant air mass flow rate test sequence. During these tests, heated water was pumped to the feed manifolds of both the spray-tubes and bank 2. The spray developed in bank 1 was used to cool the tubes of bank 2. Thus, data on the temperature history of the spray-water in bank 1 could be used to calculate local heat and mass transfer coefficients, while data on the temperature profile of the bank 2 tubeside flow provided

information necessary for the calculation of overall heat transfer coefficients.

An additional datum for these tests was the bank 2 tubeside mass flow rate, W_T . Since no taps had been provided in the tubes of bank 2 to measure this variable, but it was found that the manometers were unreliable. It was therefore decided to determine the tubeside mass flow rate by an energy balance method applied to single-phase heat transfer data.

Heated water was pumped through bank 2 and the mass flow rate in each tube indicated, but not specified, by the height of fluid in the bank 2 manometers. This level was held constant while heat transfer took place between the tubeside flow and air. Three tests were made, one test at each of the air mass flow rates to be used in the constant air mass flow rate tests. The input and output temperatures of air and tubeside fluid were recorded by thermocouples placed in the tube banks and the bank 2 manifolds respectively. Since the air mass flow rate was known, the tubeside mass flow rate could be calculated.

During the subsequent two-phase tests, the tubeside flow was maintained at the known level determined by the single-phase tests. In most other respects, the same procedure as developed for the survey tests was followed in the constant air mass flow rate tests. It was necessary, however, to employ two Honeywell recorders,

one for each tube bank, and each of these calibrated as before.

Water temperature at spray-water injection and the input and output temperatures of the tubeside flow were now measured by thermocouples placed in the manifolds of bank 2. Since the same water source was used for both the spray-tubes and the manifolds, measuring the input water temperature at the feed manifold for one system determined the input temperature for both. The relatively large size of the manifolds, as compared to the thermocouples, caused the water contained in the manifolds to act as thermal reservoirs. It was therefore necessary to pass water through the manifolds for a time sufficient to allow the entire system to reach input water temperature. This equilibrium condition was indicated by identical input and output temperatures of tubeside fluid with no heat transfer present. This procedure compared roughly to the requirement of thermal equilibrium which was imposed on the fluid meters during the survey tests.

Data Reduction

Air Mass Flow Rate. The air mass flow rates were determined by standard methods outlined in Ref. 3, page 65.

Tubeside Mass Flow Rate. The tubeside flow rate was determined by conservation of energy. The air mass

flow and the temperature changes of both the air and tubeside flow were known. Hence conservation of energy required that:

$$W_A C_A \Delta t_A = W_T C_L \Delta T \quad (4-1)$$

hence
$$W_T = W_A C_A \Delta t_A / C_L \Delta T \quad (4-2)$$

The tubeside mass flow rate was determined for each of the air mass flow rates used in the constant air mass flow rate tests and an average of the three values used in subsequent computations.

Local Heat and Mass Transfer Coefficients. The local heat and mass transfer coefficients were determined by iterative Runge-Kutta integration of equations (3-25) thru (3-28). This was done with a computer technique developed by Wright-Patterson Air Force Base Computer Center and Finlay (Ref. 6). The input data required for the calculation included spray-water and air mass flow rates, spray-water and air initial temperatures, barometric pressure, and the initial partial pressure of water vapor in the air. The spray-water temperature at the position in the heat exchanger where the coefficients were to be determined and the total heat transfer area up to that point were used as boundary conditions for the numerical integration. The equations were integrated with assumed values for H_{LA} and β

and the spray water temperature as a function of area calculated up to the area of interest. At this point the calculated and measured values of spray-water temperature were compared and if the per cent difference between these quantities was greater than a predetermined tolerance then the integration was repeated with new values for H_{LA} and β . In all cases reported, the local heat and mass transfer coefficients were computed at the exit from bank 1. The values found are shown in Tables 3 and 4, Appendix I.

Total Heat Transfer Coefficients. A total heat transfer coefficient which included the overall heat transfer coefficient (U), the local heat transfer coefficient (H_{LA}) and the local mass transfer coefficient (β) was computed by considering an energy balance on the total spray-flow through the heat exchanger. If evaporative losses of spray-water are neglected and if the spray at exit from bank 2 is assumed saturated, then a total energy balance over the heat exchanger may be written as:

Total Energy In + Heat Added = Total Energy Out (4-3)
that is:

$$W_A H_{A1} + W_L T_1 C_L + Q_{TOT} = W_A H_{Af} + W_L T_f C_L \quad (4-4)$$

or

$$Q_{TOT} = W_A (H_{Af} - H_{A1}) + W_L (T_f - T_1) C_L \quad (4-5)$$

where

HA_i = Air initial enthalpy at
ambient relative humidity

HA_f = Air final enthalpy assumed
saturated at temperature

T_f

T_i = Spray-water injection temperature

T_f = Spray-water final temperature at
exit from bank 2

With the total heat added known, a total heat transfer coefficient may be defined as:

$$H_{TOT} = Q_{TOT}/A_{TOT}\Delta T_{AVE} \quad (4-6)$$

where

A_{TOT} = Total heat transfer area of
bank 2

ΔT_{AVE} = Temperature difference between
the tubeside average temperature
and the air average temperature

The total heat transfer coefficients are shown in Table 5, Appendix I.

Amplification Factor. The total heat added was also used to compute a two-phase amplification factor, (AF). This number represents the amplification which is achieved in the single-phase heat flux when water spray is introduced into an air stream. The single-

phase tests used to determine the tubeside mass flow rate also provided data needed to compute the heat transferred to the air. The ratio of the two-phase total heat flux to single-phase heat flux at the same air mass flow rates, determined the amplification factor. Amplification factors are shown in Table 6, Appendix I.

Overall Heat Transfer Coefficients. The overall heat transfer coefficient was given by (3-13) as:

$$\frac{1}{U} = \frac{1}{H_{LT}} + \frac{1}{H_W} + \frac{1}{H_{TL}} \quad (4-7)$$

Eckert, et al (Ref. 2) has reported that the convective heat transfer coefficient between the tubeside flow and the tube wall may be given by a relation of the form:

$$H_{LT} = \frac{CK_L}{OD} Re_T Pr (0.00037 + 0.00926 (Re_T)^{-0.269}) \quad (4-8)$$

where

Re_T = Tubeside Reynolds number based
on the tube inner diameter

Pr = Tubeside Prandtl number

K_L = Water Thermal Conductivity

OD = Tube outer diameter

C = Constant

The effective convective heat transfer coefficient through the tube wall is based on Fourier's law and defined as:

$$H_W = KW/OD \ln(OD/ID) \quad (4-9)$$

The only component for the overall heat transfer coefficient which remains undefined is the convective heat transfer coefficient from the outer tube surface to the shellside liquid, H_{TL} . Observations of two-phase flow indicated that after the first few rows of tubes, the dispersed droplet flow became more aggregate. Thus it was assumed that an empirical relation for convective heat transfer coefficients from liquids to cylinders in cross flow could be used to approximate H_{TL} . Holman (Ref. 9, page 170) describes a relation of this form as:

$$H_{TL} = \frac{K_L}{OD} (0.35 + 0.56(Re_L)^{0.52}) Pr^{0.3} \quad (4-10)$$

where

Re_L = Shellside Reynolds number based
on tube outer diameter.

K_L = Water thermal conductivity

OD = Tube Outer Diameter

Pr = Water Prandtl number

The only remaining unknown in the relation for the overall coefficient is the constant C in relation (4-8). Finlay (Ref. 6) suggested that this term be determined by linear regression applied to single-phase heat transfer data. The overall coefficient for air alone is given as:

$$\frac{1}{U_{SP}} = \frac{1}{H_{LT}} + \frac{1}{H_W} + \frac{1}{H_A} \quad (4-11)$$

In this situation, the convective heat transfer coefficient between the tube and shellside fluid is replaced by a convective coefficient between the tube and air, H_A . McAdams, (Ref. 11 page 272) has reported that this coefficient is given as:

$$H_A = B(Re_A)^S K_A / OD \quad (4-12)$$

where

B, S = Constants dependent on tube
bank geometry

Re_A = Air Reynolds number based on
velocity at the minimum flow
area and tube outer diameter.

K_A = Air Thermal conductivity

OD = Tube outer diameter

Equation (4-11) can be written in the form:

$$\frac{1}{U_{SP}} - \frac{1}{H_W} = \frac{1}{H_{LT}} + \frac{1}{H_A} \quad (4-13)$$

From equation (4-8) let

$$F = K_L Re_T Pr (0.00037 + 0.00926 (Re_T)^{-0.269}) \quad (4-14)$$

then

$$\frac{1}{U_{SP}} - \frac{1}{H_W} = \frac{1}{CF} + \frac{1}{H_A} \quad (4-15)$$

and

$$F \left[\frac{1}{U_{SP}} - \frac{1}{H_W} \right] = \frac{1}{C} + \frac{F}{B(Re_A)^S} \frac{K_A}{OD} \quad (4-16)$$

Equation (4-16) is of the form $y = mx + b$

where

$$y = F \left[\frac{1}{U_{SP}} - \frac{1}{H_W} \right]$$

$$x = FOD / (Re_A)^{S_{K_A}}$$

$$m = 1/C$$

$$b = 1/B$$

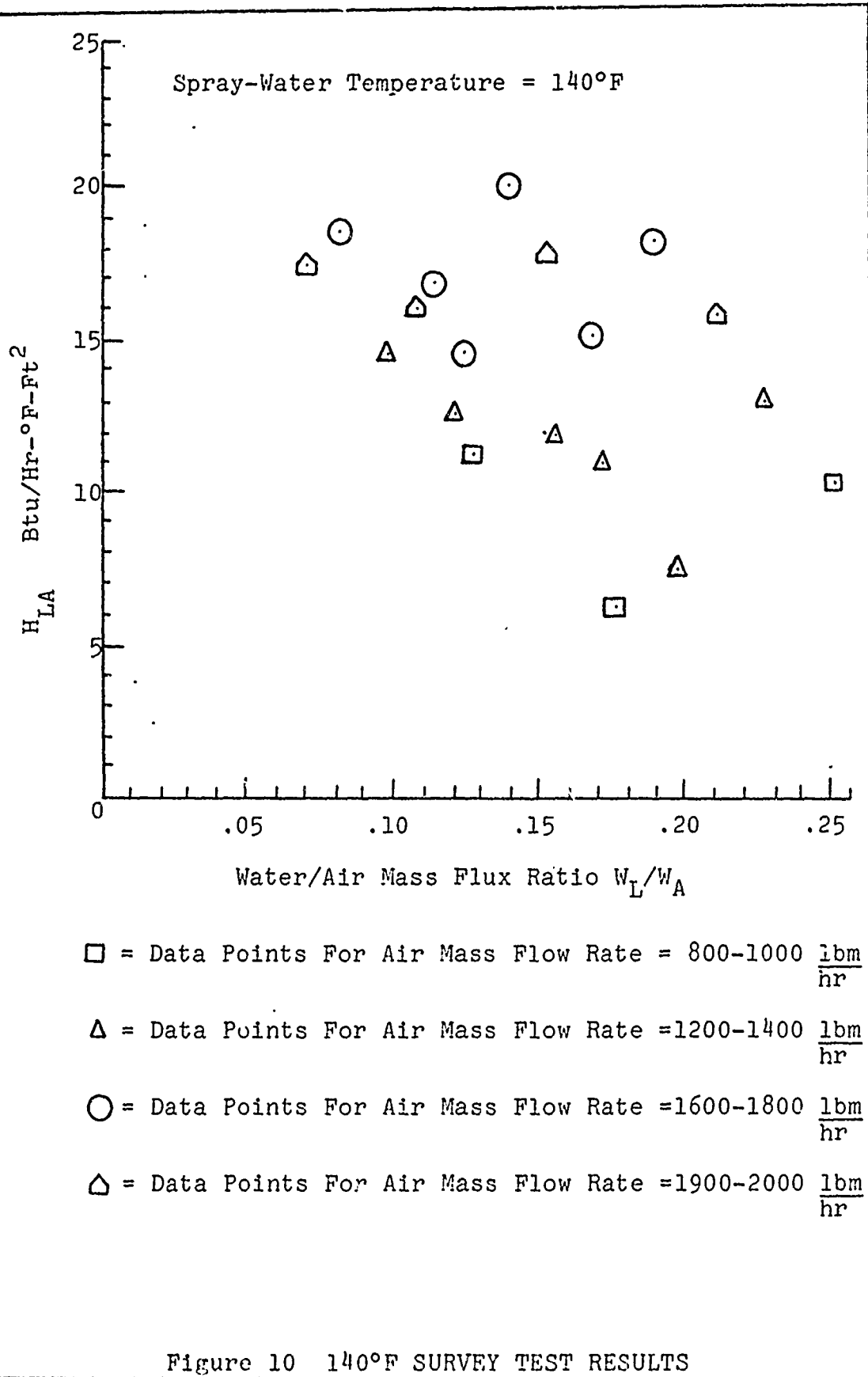
U_{SP} was determined from single-phase data ($U_{SP} = Q/A\Delta T$) and values for x and y were found. These ordered pairs were subjected to a least-squares fit and the value of C determined. With the final constant known (4-7) was solved to determine U .

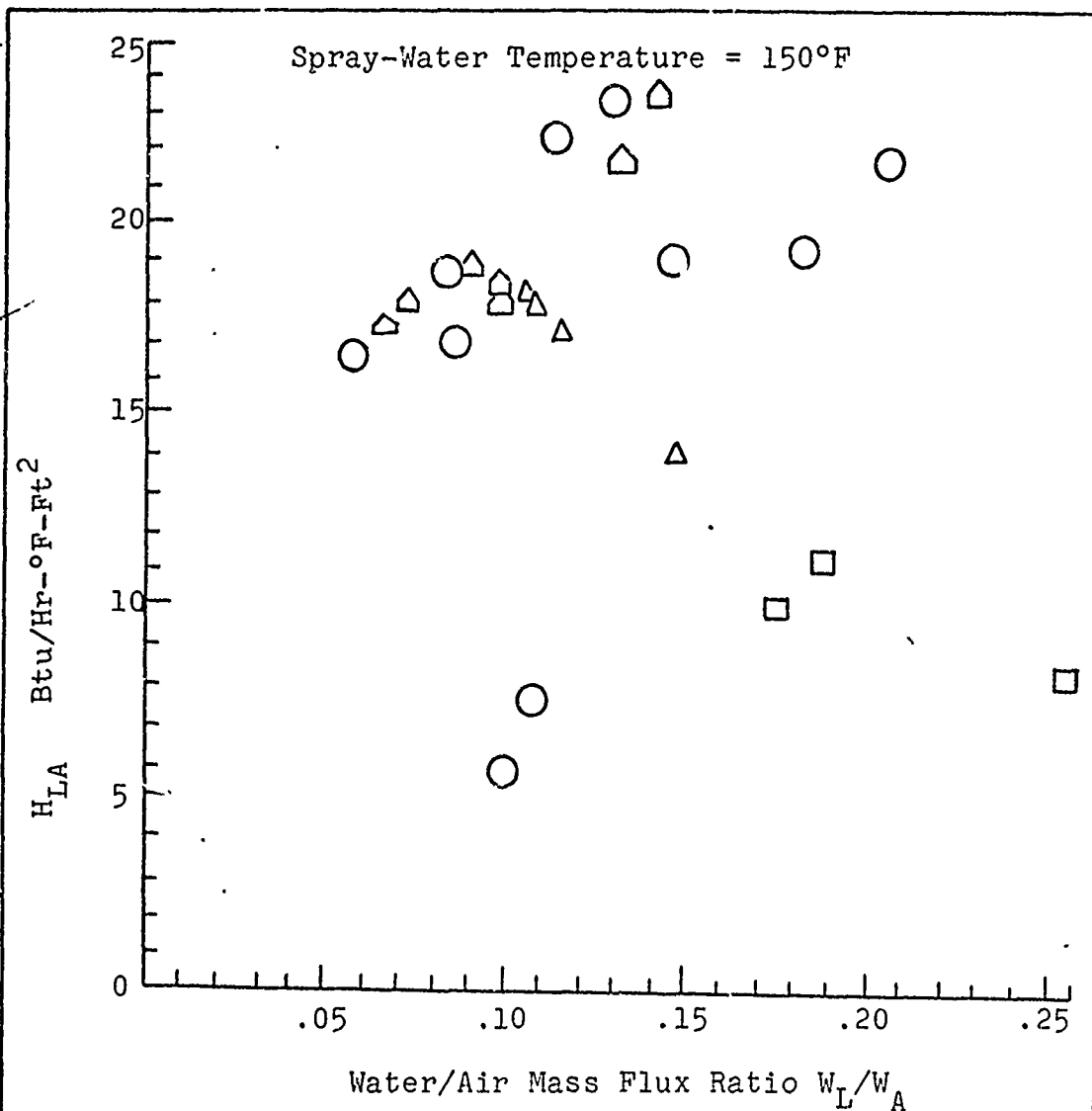
V. Results and Discussion

The values for local heat transfer coefficients obtained during the survey tests are plotted against mass flux ratio in Figures 10, 11, and 12. The scatter found in these plots is due to the superposition of data from tests at different air mass flow rates. Initial attempts at comparison of these data were fruitless until the data points were grouped into different classes on the basis of air mass flow rates. This was done in order to separate the points and determine the characteristics of the plot. The groupings used in each case are shown on the appropriate figures.

The data plot of Figure 11 indicates a maximum value for the local heat transfer coefficient which occurs in the lower mass flux ratio range. As the mass flux ratio increases, scattering in the data points becomes more evident. This is believed due to instabilities in the two-phase flow pattern which are enhanced at higher mass flux ratios. As more water is injected, the tendency for spray-water to flow in sheets or slugs of fluid increases. This in turn introduces wide variations in the temperatures sensed by the thermocouples.

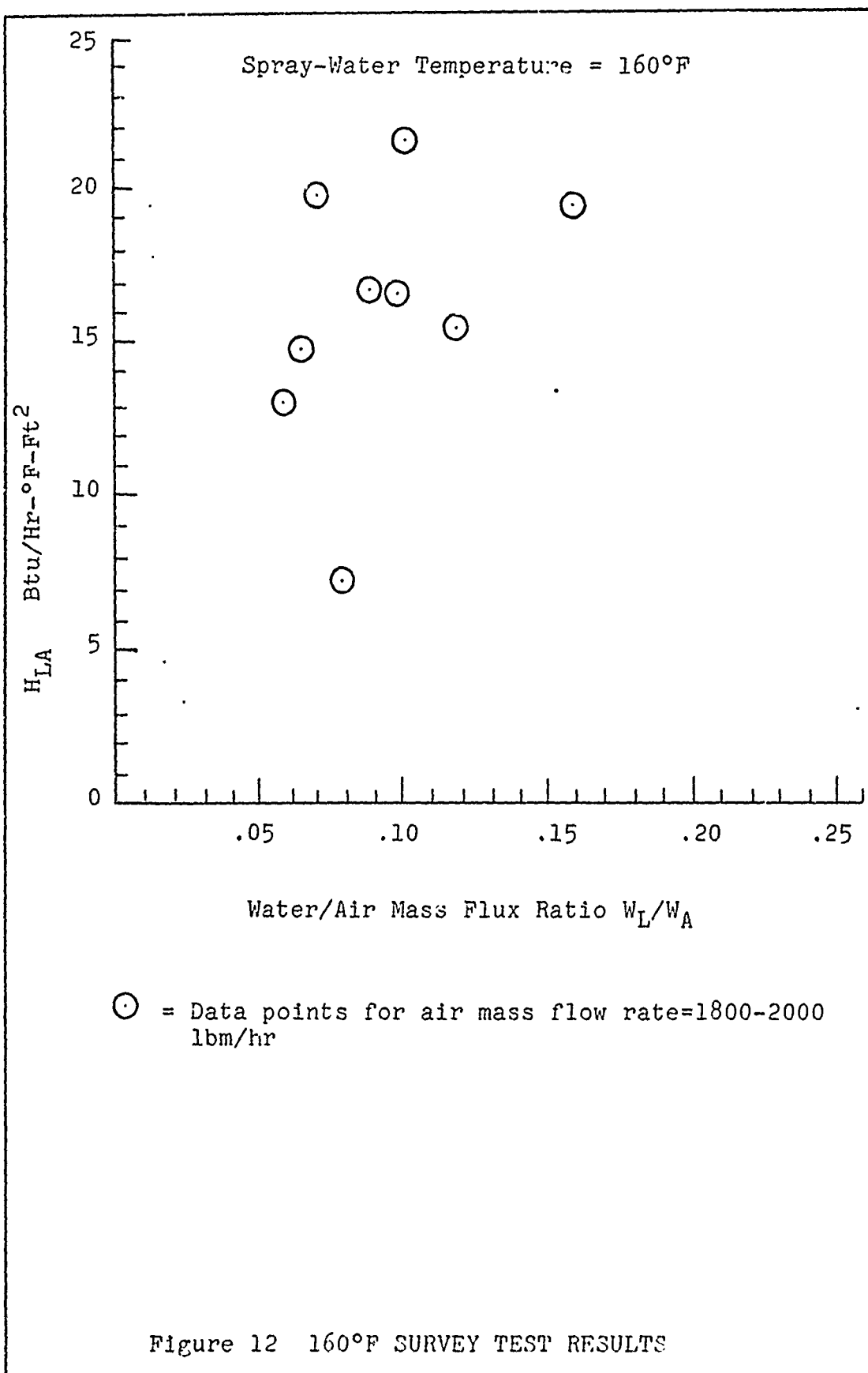
The dependence of local heat transfer coefficients on air mass flow rates and air Reynolds number is more apparent in the data plots for constant air mass flow rate tests at 140° F. These data plots from this test





- = Data Points For Air Mass Flow Rate = 800-1000 $\frac{\text{lbm}}{\text{hr}}$
- △ = Data Points For Air Mass Flow Rate = 1200-1400 $\frac{\text{lbm}}{\text{hr}}$
- ▵ = Data Points For Air Mass Flow Rate = 1600-1800 $\frac{\text{lbm}}{\text{hr}}$
- = Data Points For Air Mass Flow Rate = 1900-2000 $\frac{\text{lbm}}{\text{hr}}$

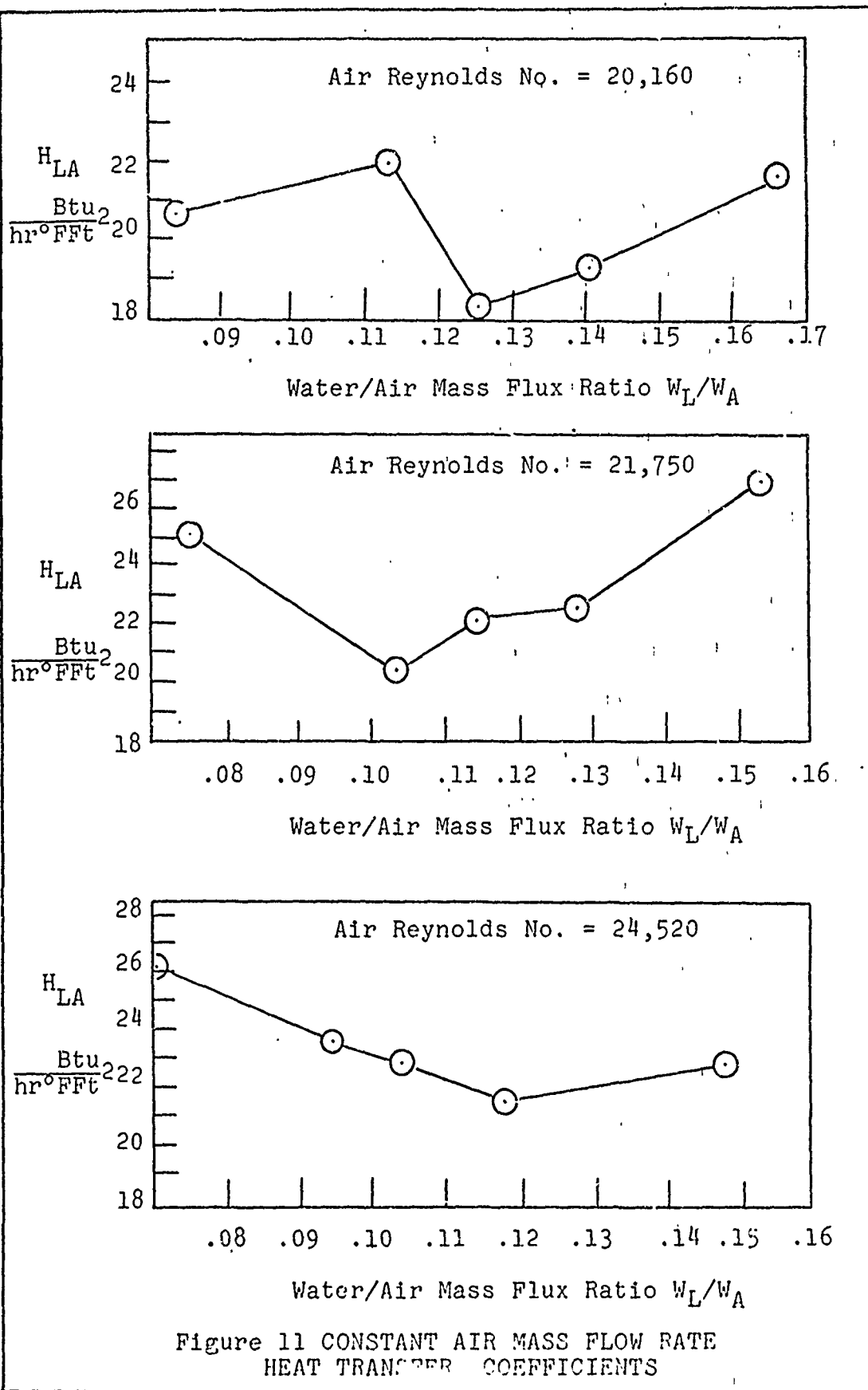
Figure 11 150°F SURVEY TEST RESULTS



series are shown in Figure 13. The curves are similar, with single maximum and minimum points indicated in each. However, as the air Reynolds number increases, the values of the maxima and minima increase also. This trend has been interpreted to imply a direct relationship between air Reynolds number and local heat transfer coefficient. In addition to the upward shift in coefficient value, however, the mass flux ratio at which the indicated maximum occurs is lowered. This implies that spray-flow heat transfer is most efficient at high air mass flow rates, where water droplets are more readily carried along the air streamlines from tube to tube.

Comparison of the local heat transfer coefficients determined in both test sequences indicates that the coefficients from the constant air mass flow rate tests are generally higher than those of the survey test sequence. The reason for this increase is unknown, but it may be that recirculation from bank 2 during the constant air test contributed to the higher values found.

The values of the mass transfer coefficients are tabulated in Tables 3 and 4, Appendix I. Since these coefficients are related to the heat transfer coefficients by a constant, the variation in the mass transfer coefficients with mass flux ratio and air Reynolds number are identical in form, if not value, to those observed for the heat transfer coefficients.



Overall Heat Transfer Coefficients

The values of the component terms in the overall coefficients and the resultant overall coefficients are tabulated in Table 5, Appendix I. Because of the analog used to compute the overall coefficients, the smallest of the three components, the convective heat transfer coefficient between the tubeside flow and the tube-wall, becomes the dominant term. This coefficient is a function of the tubeside mass flow, and is nearly constant. Only variations in property values, which were evaluated at the average tubeside temperature for each test, influenced the value of this term.

The convective heat transfer coefficient between the tube outer wall and the shellside flow is a function of the shellside Reynolds number. Hence the coefficient varies with mass flowrate. The wall conductive heat transfer coefficient is constant and very large as compared to the other terms, and in the model used may be neglected. Because of the dominance of the tubeside flow/wall coefficient, the overall heat transfer coefficient was found to be nearly constant. The average value found was $13.88 \text{ Btu/hr-}^\circ\text{F-ft}^2$.

Total Heat Transfer Coefficients

The total heat transfer coefficient and the total heat added are tabulated in Table 6, Appendix I. Any

maximums in the values of these quantities were not apparant, and these values simply increase as mass flux ratio increases.

VI. Conclusions

The experimental technique developed for the constant air mass flow rate tests more clearly delineated the functional dependence between the local heat transfer coefficients, mass flux ratios, and air Reynolds numbers. As the air Reynolds number increased, the mass flux ratio at which the local heat transfer coefficient reached its maximum value decreased. From this result it was concluded that spray-flow heat transfer was more efficient at higher air mass flow rates, where the entrained water droplets were more readily carried from tube to tube.

The overall heat transfer coefficients were found to be nearly constant in value and primarily determined by the convective heat transfer coefficient between the tubeside flow and the tube wall. Since the overall coefficient included a factor determined by the convective heat transfer coefficient between the outer tube wall and the shellside flow, some small variation in the overall heat transfer coefficient resulted with changing shellside Reynolds numbers. However, as a result of the dominance of the tubeside coefficient, it was concluded that the presence of spray-flow did not significantly change the overall coefficient.

Unlike the local heat transfer coefficient, the total heat transfer coefficients did not display any

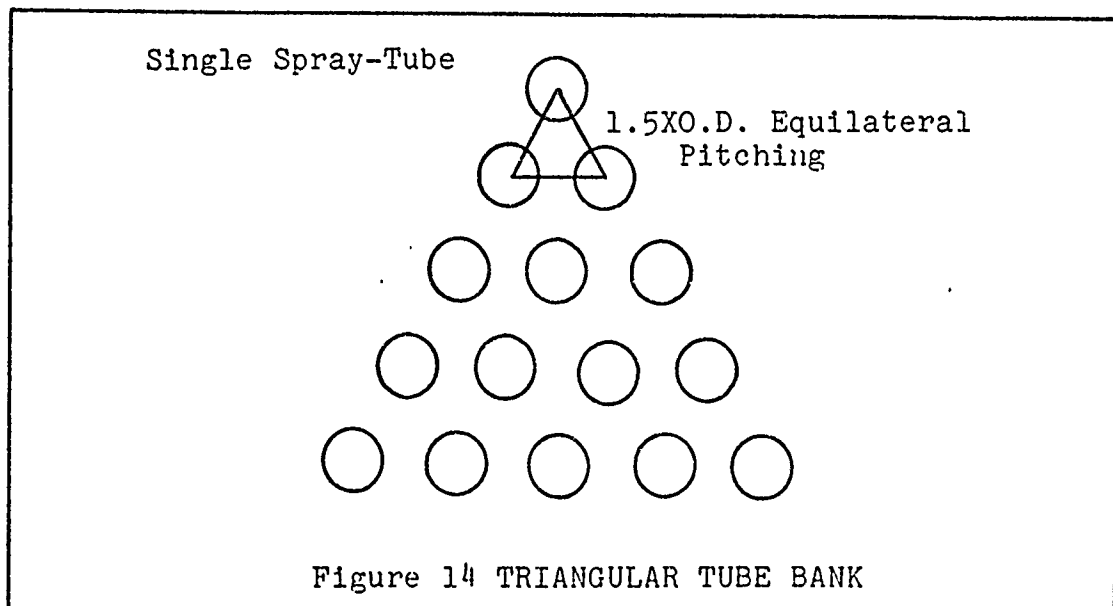
GNE/PH/72-2

identifiable dependence on mass flux ratio or air Reynolds number. Therefore, no conclusions were reached regarding any functional relationship between these coefficients and other experimental parameters.

VII. Recommendations for Further Study

The existing apparatus should be modified to allow for observation of the two-phase flow pattern. The modifications should include the installation of windows or ports in the entrance diffuser to permit visual observation of the spray injection across the heat exchanger. The injection of spray was assumed uniform in both the longitudinal and transverse directions but this could not be confirmed.

Consideration should be given to constructing a smaller tube bank to allow observation of the droplet paths in their passage from tube to tube. This could be done by constructing a triangular tube bank as shown in Figure 14.



Such a bank would incorporate the same 1.5XO.D. pitching used before but would be limited to a single spray-tube at the triangle apex. This would also limit operation to lower mass flux ratios.

At the end of the test series, the spray-tubes were examined and found to be badly clogged with scale. It is recommended that in future tests two sets of spray-tubes be used, and that these be rotated and cleaned periodically to insure uniform spray injection.

Experiments should be conducted in which different combinations of spray-tubes were used. The bank could be operated with all seven tubes and then the end tubes turned off. On the other hand, the center tube could be operated alone and then additional tubes on either side of the center brought into operation. This process would continue until all seven tubes were operating. If such tests were conducted at a constant total spray-water mass flow rate, some light could be shed on the flow pattern in tube bank 1.

The manifold valve in bank 2 should be repositioned in front of the input manifold. In their present position they do not exert control on the flow in a single tube but merely increases the entire system pressure. It is believed that in the proposed position the tubeside mass flow rates in the individual tubes of bank 2 could be controlled. A means of measuring the

total tubeside mass flow rate is necessary. It is believed that an orifice meter placed in the line to the bank 2 feed manifold would suffice for this purpose.

It is recommended that the constant air mass flow rate test procedure be used to determine local and total coefficients for higher air mass flow rates than used here.

Bibliography

1. Acrivos, A., J.E. Ahern, and A.R. Vagy. Research Investigation of Two Component Heat Transfer. ARL 64-1161. Wright-Patterson Air Force Base, Ohio: Aerospace Research Laboratory, 1964.
2. Allen T.W. and E.R.G. Eckert. "Friction and Heat Transfer Measurements to Turbulent Pipe Flow of Water (Pr=7 and 8) at Uniform Wall Heat Flux." Transactions of ASME, Vol. 86, No. 3, pp. 301-310, Aug 1964.
3. American Society of Mechanical Engineers. Fluid Meters Their Theory and Application (Fifth Edition). New York: ASME, 1959.
4. Elperin, I.T. "Heat Transfer of Two-Phase Flow With a Bundle of Tubes." Inzhenerno-Fizicheskii Zhurnal, Vol. IV, No. 8, pp. 30-35, Aug 1961.
5. Finlay, I.C. and T. McMillan. Pressure Drop, Heat and Mass Transfer During Air/Water Mist Flow Across a Bank of Tubes. NEL Report No. 474, Glasgow, Scotland: National Engineering Laboratory, 1970.
6. Finlay, I.C. "Notes on the Design of Spray-Flow Rig." Unpublished Manuscript. Aerospace Research Laboratory, Wright-Patterson Air Force Base Ohio: Department of Thermomechanics, 1970.
7. Hodgson and Sunderland. "Heat Transfer From a Spray-Cooled Isothermal Cylinder." Transactions of ASME, Vol. 7, No. 4, pp. 567-572, 1968.
8. Hoelscher, J.F. Study of Heat Transfer from a Heated Cylinder in Two-Phase, Water-Air Flow. AFIT Thesis 1965.
9. Holman, J.P. Heat Transfer (Second Edition). New York: McGraw-Hill Book Company, Inc., 1968.
10. Holman, J.P. Thermodynamics. New York: McGraw-Hill Book Company, Inc., 1969.
11. McAdams, W.H. Heat Transmission (Third Edition). New York: McGraw-Hill Book Company, Inc., 1954.

Bibliography Continued

12. Smith, J.E. "Heat Transfer Studies of Water-Spray Flows," Northern Research and Engineering Corporation. ARL 66-0091. Wright-Patterson Air Force Base, 1966.
13. Strock, C. Handbook of Air Conditioning Heating, and Ventilating. New York: The Industrial Press, 1959.
14. Takahara, E.W. Experimental Study of Heat Transfer From a Heated Circular Cylinder in Two-Phase, Water-Air Flow. AFIT Thesis, 1966.

Appendix I

Experimental Results
in Tabular Form

Table 1 SURVEY TEST PARAMETER RANGE

Water Temperature = 140° F		Water Temperature = 150° F		Water Temperature = 160° F	
W_L (lbm/hr)	W_A (lbm/hr)	MFR	W_L (lbm/hr)	W_A (lbm/hr)	MFR
140	2018	.069	120	2056	.058
140	1598	.082	120	1870	.064
140	1447	.097	120	1704	.070
140	1278	.110	163	2057	.079
140	1102	.127	140	1420	.099
140	800	.175	140	1255	.112
210	1859	.113	140	1055	.133
210	1678	.125	140	806	.174
210	1363	.154	163	1870	.087
210	1243	.169	163	1711	.095
210	1073	.196	180	2059	.087
210	841	.250	180	1887	.095
280	1846	.139	180	1710	.105
280	1996	.152	210	2165	.097
280	1677	.167	210	2016	.104
280	1241	.226	210	1452	.145
350	1674	.188	210	1131	.186
350	2007	.209	210	830	.253
			240	2061	.116
			240	1888	.127
			240	1712	.140
			280	2066	.136
			280	1936	.145
			350	1936	.181
			420	2076	.202
			108	1817	.060
			120	1818	.066
			140	2065	.068
			163	1819	.090
			180	1817	.099
			210	2063	.102
			210	1743	.120
			280	2065	.136
			280	1747	.160
			350	1747	.200
			420	2067	.203

Table 2 CONSTANT AIR MASS FLOW RATE TEST PARAMETER RANGE							
Water Temperature = 125°F				Water Temperature = 140°F			
Air Reynolds No.	W_L (lbm/hr)	W_A (lbm/hr)	MFR	Air Reynolds No.	W_L (lbm/hr)	W_A (lbm/hr)	MFR
20,200	120	1690	.071	20,160	140	1680	.083
	163		.097		191		.113
	180		.107		210		.125
	202		.119		235		.140
	240		.142		280		.167
23,830	120	1870	.063	21,750	140	1813	.077
	180		.094		191		.105
	191		.104		210		.116
	235		.126		235		.130
	240		.129		280		.154
25,240	140	2110	.066	24,520	140	2044	.070
	190		.090		191		.095
	210		.100		210		.105
	236		.112		235		.120
	240		.114		280		.150

Table 3 LOCAL COEFFICIENTS FOR SURVEY TESTS

Water Temperature = 140°F				Water Temperature = 150°F				Water Temperature = 160°F			
MFR	$\frac{\beta}{\text{hr-psi-ft}^2}$	$H_{LA} \frac{\text{Btu}}{\text{hr}^\circ\text{F-ft}^2}$	MFR	$\frac{\beta}{\text{hr-psi-ft}^2}$	$H_{LA} \frac{\text{Btu}}{\text{hr}^\circ\text{F-ft}^2}$	MFR	$\frac{\beta}{\text{hr-psi-ft}^2}$	MFR	$\frac{\beta}{\text{hr-psi-ft}^2}$	$H_{LA} \frac{\text{Btu}}{\text{hr}^\circ\text{F-ft}^2}$	
.069	3.58	17.57	.058	3.54	17.4	.060	2.7	.060	2.7	13.25	
.082	3.77	18.45	.064	3.62	17.73	.066	3.06	.066	3.06	15.00	
.097	3.00	14.71	.070	3.70	18.12	.068	4.07	.068	4.07	19.95	
.110	2.48	12.81	.079	3.79	18.58	.081	1.51	.081	1.51	7.43	
.127	2.32	11.39	.099	3.77	18.46	.090	3.47	.090	3.47	17.02	
.175	1.28	6.30	.112	3.57	17.50	.099	3.43	.099	3.43	16.80	
.113	3.49	17.09	.133	3.29	16.15	.102	4.45	.102	4.45	21.81	
.125	2.97	14.57	.174	2.09	10.27	.120	3.21	.120	3.21	15.76	
.154	2.48	12.18	.087	3.89	19.04	.126	5.77	.126	5.77	28.28	
.169	2.29	11.25	.095	3.80	18.64	.160	4.02	.160	4.02	19.74	
.196	1.59	7.82	.087	3.86	18.92	.200	6.07	.200	6.07	29.77	
.250	2.15	10.54	.095	3.76	18.48	.203	9.07	.203	9.07	44.49	
.139	4.14	24.24	.105	3.67	18.01						
.152	3.76	17.99	.097	1.20	5.93						
.167	3.13	15.34	.104	1.62	7.97						
.226	2.70	13.26	.145	2.92	14.34						
.188	3.75	18.40	.186	2.36	11.58						
.209	3.22	15.82	.253	1.73	8.68						
			.116	4.68	22.94						
			.127	4.40	21.60						
			.140	4.10	20.10						
			.136	4.80	23.52						
			.145	2.94	14.46						
			.181	3.95	19.41						

Table 4 LOCAL COEFFICIENTS FOR CONSTANT AIR MASS FLOW RATE TESTS

Water Temperature = 125°F						Water Temperature = 140°F					
Air Reynolds No.	$H_{LA} \frac{Btu}{hr^{\circ}Fft^2}$	$\frac{\beta Btu}{hrpsift^2}$	MFR	Air Reynolds No.	$H_{LA} \frac{Btu}{hr^{\circ}Fft^2}$	$\frac{\beta Btu}{hrpsift^2}$	MFR	Air Reynolds No.	$H_{LA} \frac{Btu}{hr^{\circ}Fft^2}$	$\frac{\beta Btu}{hrpsift^2}$	MFR
20,220	52.74 31.42 27.70 26.80 31.02	10.77 6.77 5.66 5.47 6.33	.071 .097 .107 .119 .142	20,160	21.27 22.96 18.27 19.74 22.60	4.34 4.68 3.73 4.03 4.60	.083 .113 .125 .140 .167				
23,830	40.77 26.13 42.70 33.93 27.69	8.33 5.33 8.72 6.93 5.65	.063 .094 .104 .126 .129	21,750	24.31 20.30 21.80 22.03 26.26	5.00 4.14 4.45 4.50 5.36	.077 .105 .116 .130 .154				
25,240	35.42 36.21 56.42 36.42	7.24 7.39 11.52 7.45	.066 .090 .100 .112	24,520	25.94 23.52 23.01 21.86 22.95	5.30 4.80 4.69 4.46 4.68	.070 .095 .105 .120 .150				

Table 5 OVERALL HEAT TRANSFER COEFFICIENT COMPONENTS

SPRAY-ON HEAT TRANSFER TEMPERATURE = 125°F					
MFR	H_{LT} $\frac{\text{Btu}}{\text{hr-°F-ft}^2}$	H_W $\frac{\text{Btu}}{\text{hr-°F-ft}^2}$	H_{TL} $\frac{\text{Btu}}{\text{hr-°F-ft}^2}$	U $\frac{\text{Btu}}{\text{hr-°F-ft}^2}$	
.071	15.3388	13.093	119.482	13.58	
.097	15.0111	13.093	138.646	13.52	
.107	15.2910	13.093	145.383	13.82	
.119	15.2910	13.093	153.800	13.89	
.142	15.4560	13.093	167.370	14.13	
.063	15.1600	13.093	119.482	13.43	
.094	15.2910	13.093	145.383	13.71	
.129	15.0020	13.093	165.653	13.75	
.126	16.0510	13.093	167.370	14.62	
.066	14.7770	13.093	128.693	13.24	
.112	15.2910	13.093	165.653	13.99	

Table 6 TOTAL HEAT TRANSFER COEFFICIENTS AND AMPLIFICATION FACTORS

Table 6 TOTAL HEAT TRANSFER COEFFICIENTS AND AMPLIFICATION FACTORS							
Water Temperature = 125°F				Water Temperature = 140°F			
MFR	Q _{TOT} (Btu/hr)	AF	H _{TOT} $\frac{\text{Btu}^2}{\text{Hr}^\circ\text{FFt}}$	MFR	Q _{TOT} (Btu/hr)	AF	H _{TOT} $\frac{\text{Btu}^2}{\text{Hr}^\circ\text{FFt}}$
.071	43,522	3.05	633	.083	88,343	5.02	849
.097	45,092	3.16	635	.113	110,374	6.27	1181
.109	48,727	3.41	640	.125	97,111	5.51	1074
.119	54,238	3.80	731	.140	101,944	5.78	1146
.142	58,122	4.07	825	.167	116,681	6.62	1262
.063	47,788	2.92	615	.077	90,189	4.69	869
.094	57,196	3.50	818	.105	107,690	5.60	1085
.126	64,302	3.93	1002	.116	117,284	6.10	1212
				.130	121,271	6.30	1256
				.154	125,135	6.51	1302
.066	69,212	3.97	734	.070	92,728	4.28	857
.090	98,990	5.68	1198	.095	113,556	5.24	1113
.100	67,705	3.77	760	.105	124,936	5.77	1259
.112	66,324	3.81	763	.120	132,845	6.13	1376
.114	72,361	4.16	1017	.150	139,918	6.46	1521

Vita

Raymond A. Carpenter was born on 11 January 1943 in Joliet Illinois. After completing grade school and high school he attended Joliet Junior College. From Joliet Junior College he attended the University of Illinois. Prior to graduation he enlisted in the United States Air Force. During his tour at Barksdale Air Force Base in Louisiana he attended Louisiana Polytechnic Institute of Technology until he was accepted in the Airman's Education and Commissioning Program. While in this program he graduated from the University of Tennessee on 10 June 1970 with a Bachelor of Science degree in Nuclear Engineering. Following Officer's Training School he received his commission on 10 September 1970 and was assigned to Wright-Patterson Air Force Base where he entered the Air Force Institute of Technology.

Permanent address: 1638 Marquette Road
Joliet, Illinois
60435

This thesis was typed by Mrs. Raymond A. Carpenter.